

SolFly:
Solar Energy Tent Fly for Humanitarian Aid

A Major Qualifying Project

Submitted to the Faculty of

WORCESTER POLYTECHNIC INSTITUTE

In partial fulfillment for the

Bachelor of Science Degree

In Mechanical Engineering

By:

Olivia Jones, ME

Edward "Ted" Noyes, ME

Advised By:

Professor Fiona Levey, ME

Date of Submission:

April 25, 2019

Abstract

The goal of this project was to develop a product which met the need for off-grid electricity production that is safe, transportable, and environmentally friendly. Displaced people have a particular need for off-grid energy. As a result, this project focuses on energy production for refugee camps. The proposed design utilizes thin film solar technology attached to a weather resistant nylon fabric on a rolling spring mechanism for ease of transportation and set up. This user-friendly device serves as a protective tent fly while producing solar electricity for tent inhabitants. The background research, stages of the design process, and testing conducted in order to develop a viable prototype are discussed in this report. It was found that SolFly provides a feasible solution to energy sparsity in refugee camps and can be adapted to meet varied consumer requirements. Recommendations to maintain structural integrity of the tent are provided.

Acknowledgements

We would like to recognize the following individuals and organizations for the contributions they made to help us develop a successful and meaningful project.

Special thanks to:

WPI Faculty and Students

- Professor Fiona Levey for her guidance and support throughout the entirety of the MQP process. We could not have done this project without your help.
- Todd Keiller for his encouragement throughout the NSF sponsored I-Corps program that allowed us to pivot our design to create a useful product.
- Professor Joe Stabile and Adriana Hera for their instruction of ANSYS simulations.
- Professor David Ollinger for conducting tests with us in the wind tunnel.
- Peter Hefti for providing workshop space, tools, and instruction when needed.
- Barbara Fuhrman for acquiring all materials and supplies.
- Professor Pratap Rao and Professor Maqsood Mughal for sharing their knowledge of thin film solar technology.
- Professor Nicola Bulled and Courtney Kurlanska for sharing their experiences with projects focused on refugee assistance.
- Sylvia Thomas sewing assistance, Evan Duffy for allowing us to use his 3D printer, and Nico Vayas Tobar, Jose Shady, Nickel Lucena, Christine Zarate, Michael Savoie, Nikki Loiseau, Keeghan O’Leary, and Wesley Fisher for taking the time to participate in interviews.

I-Corps

- The National Science Foundation for funding market research and prototyping.
- Tom Witkin for mentoring us and providing contacts and resources.
- Desi Matel-Anderson for inviting us to attend the Do Tank at HSEMA and sharing her techniques for disaster assessment and problem solving.
- All other interviewees who took the time to share their knowledge and help us develop a successful product.
 - Richard Cheek, Mike Mitchell, Rich Stapleton, Andy Trapp, Alana Geary, Winifred Spillers, Bob Dubel, Zach Witkin, Andrew Belden, Todd Bianco, Michael Judge, Dwayne Breger, Francis Cummings, Adam Jacobs, Galen Nelson, Frank Gopell, and John Odell

Table of Contents

Acknowledgements	2
List of Tables	5
List of Figures	5
1.0 Introduction	8
2.0 Background	9
2.1 Demand	9
2.1.1 Climate Change	9
2.1.1 Energy with Respect to Quality of Life	9
2.1.2 Energy in Refugee Settlements	10
2.2 Solar Energy	11
2.2.1. Photovoltaic Effect	11
2.2.2 Solar Panels	13
2.2.3 Thin Film Solar Cells	13
2.2.4 Off-Grid Solar Photovoltaics	14
2.2.4.1 General Applications	14
2.2.4.2 Humanitarian Applications	15
3.0 Design	19
3.1 Market Research	19
3.1.1 Customer Interviews	19
3.1.2 Disaster Relief Workshop	19
3.2 Design Criteria	21
3.2.1 Electrical Production	21
3.2.2 Transportability	21
3.2.3 Deployment	21
3.2.4 Cost	22
3.3 Preliminary Designs	22
3.3.1 Design Constraints	27
3.3.2 Features	28
3.3.3 Materials Selection	29
3.3.2.1 Solar Cell Selection	29
3.3.2.2 Tent Fly Material Selection	31
3.3.2.3 Housing Material Selection	32
3.3.4 Modeling	33
3.3.5 Scaled Model	48
3.4 Manufacture & Shipment	50

3.4.1 Solar Panels	50
3.4.2 Tent Fly	50
3.4.3 Spring Mechanism	51
3.4.4 Housing and Connectors	51
3.4.5 Transportation	52
4.0 Analysis	53
4.1 Structural	53
4.2 Spring Mechanism	61
4.3 Electrical	64
4.4 Drag Force Calculations	66
5.0 Testing	71
5.1 Static Load Deflection	71
5.1.1 Purpose	71
5.1.2 Materials	71
5.1.3 Procedure:	71
5.1.4 Data	71
5.1.5 Results	71
5.1.6 Conclusion	71
5.2 Spring Constant and Tension	72
5.2.1 Purpose	72
5.2.2 Materials	72
5.2.3 Procedure	72
5.2.4 Data	72
5.2.5 Results	73
5.2.6 Conclusion	73
5.3 Wind Force on Tent Fly	73
5.3.1 Purpose	73
5.3.2 Materials	74
5.3.3 Procedure	75
5.3.4 Data	75
5.3.5 Results	76
5.4 Electrical	77
5.4.1 Purpose	77
5.4.2 Materials	77
5.4.3 Procedure	78
5.4.4 Data	78
5.4.5 Results	81
5.4.6 Conclusion	83

6.0 Conclusions & Recommendations	84
7.0 Works Cited	86

List of Tables

Table 1. Energy Requirements per 60 Minutes	21
Table 2. Product Specifications for Each of the Solar Panels	29
Table 3. Solar Cell Design Traits with Respect to Area	30
Table 4. Solar Cell Design Matrix	30
Table 5. Comparison of Housing Material Options	32
Table 6. Specifications per Number of Solar Panels	66
Table 7. Drag Forces at Various Velocities	67
Table 8. Cost Analysis for Namibia	68
Table 9. Cost Analysis for Jordan	68
Table 10. Static Deflection Data	71
Table 11. Spring Data	72
Table 12. Results of Spring Constant Test	73
Table 13. Wind Tunnel Data	75
Table 14. Solar Data Day 1	79
Table 15. Solar Data Day 2	80
Table 16. Solar Data Day 3	81

List of Figures

Figure 1: LEI vs. HDI	9
Figure 2: Map of Lambert Energy Index by country	10
Figure 3: Graphical Depiction of Displaced People in 2018 According to UNHCR	10
Figure 4: Photovoltaic Effect	11
Figure 5: Band Gap and Efficiencies of Common Solar Semiconductors	12
Figure 6: Visible Light Spectrum Wavelengths	13
Figure 7: From Left to Right: Portable Solar Charger, Solar-Powered Speaker, and Solar Lantern	14
Figure 8: Military Grade Folding Solar Panels	15
Figure 9: Military Solar Energy Tent Shield	15
Figure 10: Solar Lamps	16
Figure 11: Case Portable Solar	16
Figure 12: Transportable Solar	16
Figure 13: Za'Atari Refugee Camp Solar Grid	17
Figure 14: Eco Capsule Off-Grid Home	18

Figure 15: Photo from DO Tank at HSEMA	20
Figure 16: Rotating Canopy	22
Figure 17: Awning Design 1	23
Figure 18: Awning Design 2	23
Figure 19: Palmbrella Energy & Shade System	24
Figure 20: Solar Energy Water Collector	25
Figure 21: Center Pole Tent Addition	26
Figure 22: SolidWorks Model of SolFly Design with Four Solar Panels	27
Figure 23: Side View of UNHCR “Family Tent for Hot Climate”	27
Figure 24: Solar Resource Map: Global Horizontal Irradiation	28
Figure 25: Concept SolidWorks Model of One SolFly on UNHCR “Family Tent for Hot Climate”	29
Figure 26: F-WAVE Flexible Solar Cells Diagram	31
Figure 27: Power Generation over time of F-WAVE Flexible Solar Cell Compared to Crystalline Solar Cell	31
Figure 28: Spring Mechanism Assembly Model in SolidWorks	33
Figure 29: Drawing of Spring Mechanism Subassembly: Exploded View with Bill of Materials	34
Figure 30: Drawing of Rod	35
Figure 31: Drawing of Helix Spring	36
Figure 32: Drawing of Connector A	37
Figure 33: Drawing of Pin	38
Figure 34: Drawing of Connector B	39
Figure 35: Drawing of Axle	40
Figure 36: Drawing of Container Tube	41
Figure 37: Drawing of Housing with Fly Subassembly with Bill of Materials	42
Figure 38: Drawing of Housing	43
Figure 39: Drawing of Fly	44
Figure 40: Drawing of Cap	45
Figure 41: Drawing of Cap 2	46
Figure 42: Drawing of Solar Panel	47
Figure 43: Schematic of the Circuit Design with Four Panels	48
Figure 44: Scaled SolFly Model	48
Figure 45: Optimization of Connector Design for 3D Printing	49
Figure 46: Schematic of Model Solar Circuit	49
Figure 47: F-WAVE Solar Cell Manufacturing Facility in Kumamoto, Japan	50
Figure 48: Injection Molding Machine	51
Figure 49: Schematic of Center Beam with Three Fixed Supports, COM, and Distributed Weight	53
Figure 50: ANSYS Results for Tent Beam Deflection with SolFly	58
Figure 51: Reinforced ANSYS Results for Tent Beam Deflection with SolFly	59

Figure 52: Diagram of Torque	62
Figure 53: World Insolation Map Showing Average Hours of Sunlight Per Day	65
Figure 54: Graph of Drag Force vs. Velocity	67
Figure 55: Cost Analysis for Refugee Camp in Namibia	69
Figure 56: Cost Analysis for Refugee Camp in Jordan	69
Figure 57: Diagram of Steel Frame with Nylon Fly Fabric Attached inside Wind Tunnel	73
Figure 58: Steel Frame with Nylon Fly Fabric Attached inside Wind Tunnel	73
Figure 59: F-Wave Solar Panel	77
Figure 60: Model Solar Panel	77
Figure 61: Klein Multimeter	78
Figure 62: F-Wave Wattage vs. Time	82
Figure 63: Model Circuit Wattage vs. Time	82
Figure 64: Chart of Wattage Production and Power Requirements of Devices	83
Figure 65: The Team at Project Presentation Day	85
Figure 66: SolFly Scaled Model	85

1.0 Introduction

As the human population increases, so does the global demand for energy. Increased energy production is needed in both industrialized and developing nations alike. The demand for electricity that can be easily transported and installed is especially prevalent in situations where people are displaced from their homes, such as refugees and natural disaster victims. Though aid organizations such as the UNHCR successfully provide shelter to displaced peoples, it is reported that 90% of refugees in camps do not have access to light [9]. In modern day, electricity is considered a basic human need. The limited energy sources currently available to these populations threaten the global environment. Generator-dependent camps rely on fossil fuel, a primary contributor to climate change. Innovations within the renewable energy sector are necessary to meet energy demands in refugee camps while limiting environmental impact. The team identified this as a market gap that could be filled by new product development. The necessary background research, design analysis, prototyping, and testing to create such a product are discussed in this report.

2.0 Background

2.1 Demand

2.1.1 Climate Change

Climate change has been a growing issue for many years, and is a factor for consideration in all industries. The Paris Climate Change agreement was established at the UN Climate Change Conference in 2015 to prevent catastrophic impacts on global environments as result of rising temperatures. This agreement proposed temperature limits at which these effects would be realized ranging from +1.5° C to +2° C. One estimate is that, when the 1.5° C increase mark is reached, the population exposed to water scarcity will increase by 271 million [19]. Global warming has begun, and will no doubt continue to play a large part in the world economy and dictate industry standards across the globe. As such, the renewable energy industry is constantly expanding its scope of influence and initiative.

2.1.1 Energy with Respect to Quality of Life

Quality of life is influenced by access to electricity. A 2012 study conducted for the UK Department for International Development indicates the correlation between energy and quality of life. The Lambert Energy Index (LEI) is a statistical combination of Energy Return on Investment, energy use per capita, and Gini Index of income distribution. As shown in Figure 1, higher LEI values corresponded with higher Human Development Index (HDI) values by country. The HDI increases with quality of life and considers factors including life expectancy, education, and per capita income [15]. The variation by country of LEI values is shown in Figure 2.

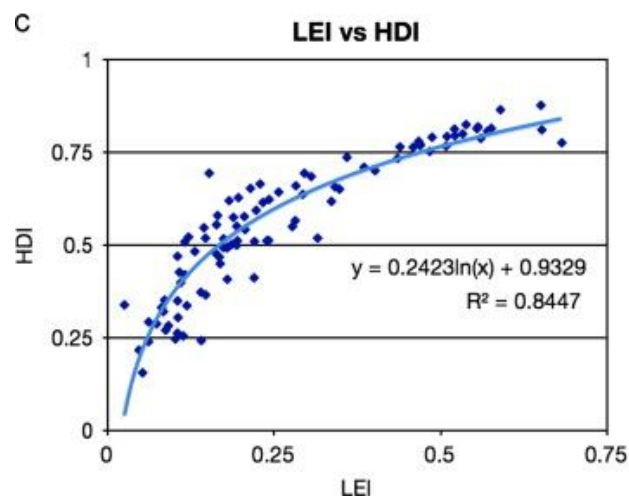


Figure 1: LEI vs. HDI [15]

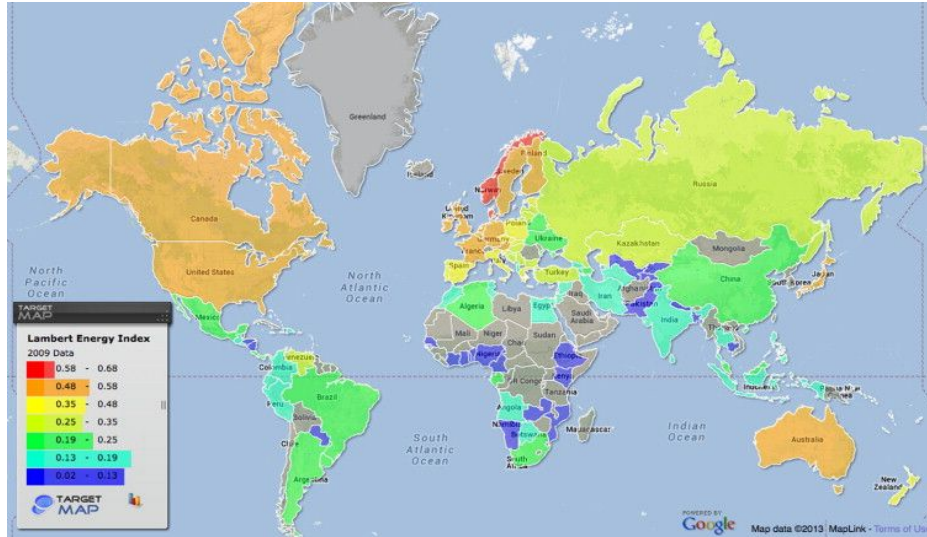


Figure 2: Map of Lambert Energy Index by country [15]

2.1.2 Energy in Refugee Settlements

The United Nations High Commissioner of Refugees (UNHCR) is an agency created with a mandate to protect refugees, forcibly displaced communities, and stateless persons, and assist in their resettlement, local integration or repatriation to their home country. Across the globe there are 68.5 million forcibly displaced persons and 25.4 million refugees, and 57% of them come from South Sudan, Afghanistan and Syria [33]. The UNHCR is currently involved with 19.9 million refugees. Refugees are spread across a multitude of climates. As a result, the UNHCR has shelter protocol for a variety of climates.

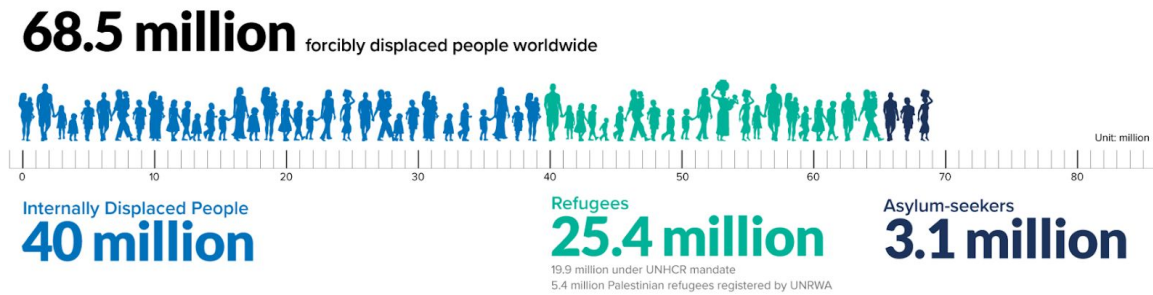


Figure 3: Graphical Depiction of Displaced People in 2018 According to UNHCR [33]

Though shelters are designed for a range of regions, refugee settlements often have limited or no electricity access. Refugees face the numerous hardships associated with lack of access to this resource. Green states that, based on UNHCR data on refugees in camps, nine out of ten refugees do not have access to light [9]. Connection to the grid is not feasible due to remote location or insufficient funds. In these cases, forcibly displaced persons are dependent primarily on energy sources such as firewood, charcoal, liquified petroleum gas (LPG), and

diesel fuel for cooking and lighting [16]. The high cost, yet low quality nature of these energy sources creates financial burdens, social repercussions, health and safety risks, and environmental impacts.

Records show the UNCHR spends about \$100 million on diesel fuel every year [9]. One study conducted by researchers from the Royal Institute of International Affairs, estimates that the introduction of solar lamps and improved cookstoves in camps could save \$303 million in energy costs annually [16]. Beyond cost, the current methods of energy use have major social impacts. Lack of ample lighting limits operable hours for workers and students and therefore inhibits workforce potential. Public lighting also improves community safety for refugees travelling across camps at night [9]. Other safety risks include illegal electrical connections, open fires, and candles which pose fire hazards that can be disastrous to shelters in close proximity. Reliance on biomass fuel also puts people at risk for exposure to pollutants indoors [16]. This can result in health complications for displaced families. With respect to environmental concerns, an estimated 14.3 million metric tons of CO₂ were emitted by displaced households alone in 2014, from all fuel types [16]. More efficient energy supplies would decrease these emissions while increasing energy production. The UNHCR believes that introduction of renewable energy to refugee camps would “diminish the conflict that arises from competition over natural resources, but would also energize the renewable energy market in those impoverished regions.” [13]

2.2 Solar Energy

Solar energy technology is versatile because it can be implemented wherever there is exposure to sunlight. Solar energy is most commonly collected through panels comprised of photovoltaic cells, but panels are only one variation of solar energy collection. One progressive technology is thin film solar cells which can be applied to more varied situations than traditional panels due to their lightweight, flexible design.

2.2.1. Photovoltaic Effect

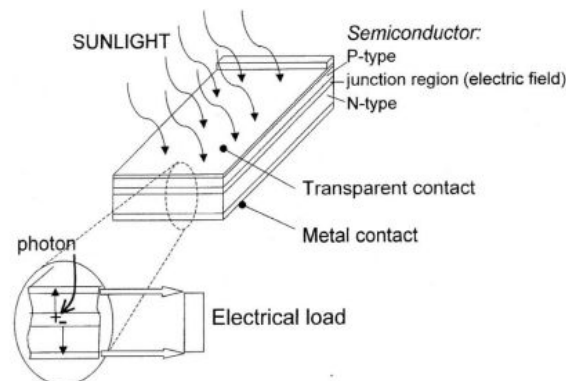


Figure 4: Photovoltaic Effect [25]

The Photovoltaic (PV) effect is the process by which energy from sunlight is harnessed for conversion into electricity. Discovered in 1839 by Alexandre Edmund Becquerel, this process, illustrated in Figure 3, is the underlying science behind existing solar energy technology [25]. The process works through photons emitted by sunlight coming into contact with a semiconductor material within the solar cell. Photons ionize the semiconductor and release electrons which produce an electric current [20]. The term bandgap is the term used to describe the energy difference between the valence and conduction bands. Materials with a small bandgap are semiconductors and those with a large bandgap are insulators. Because solar cells must be able to absorb the most amount of light while containing the most voltage, a bandgap between 1 and 1.7 eV is ideal for solar semiconductors. Common semiconductor materials used in solar cells and their corresponding conversion efficiencies are shown in the figure below [5].

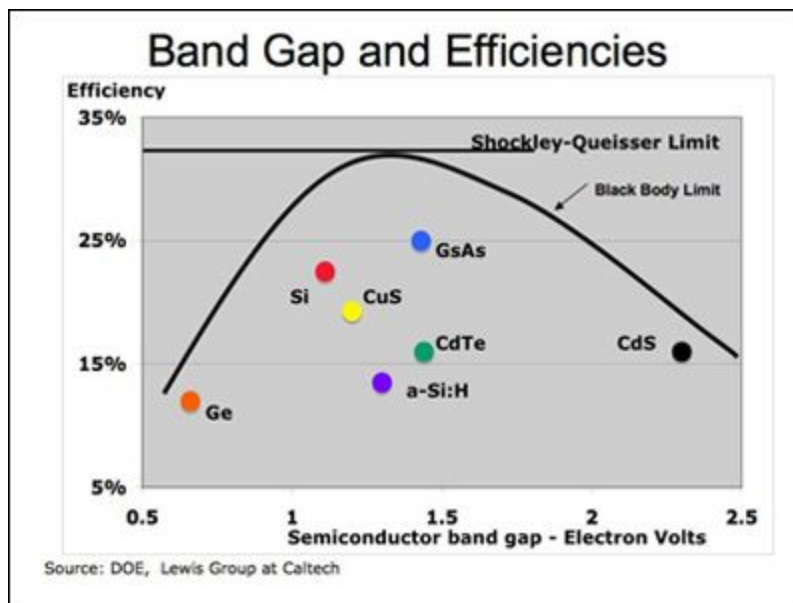


Figure 5: Band Gap and Efficiencies of Common Solar Semiconductors [5]

Solar cell efficiency is the percentage of energy from sunlight that is effectively converted to electrical energy. Remaining energy that is not converted, is lost by heat and photons passing through the cell. Solar efficiency is limited by the rays of light because different wavelengths create different types and amounts of energy. Visible waves are able to dislodge electrons and produce a current. As shown in the figure below, visible waves range 380 nm to 750 nm. Infrared rays do not have enough energy to produce a current, and ultraviolet rays produce heat rather than electricity [25]. Some other factors that affect conversion efficiency are temperature and reflection [20].

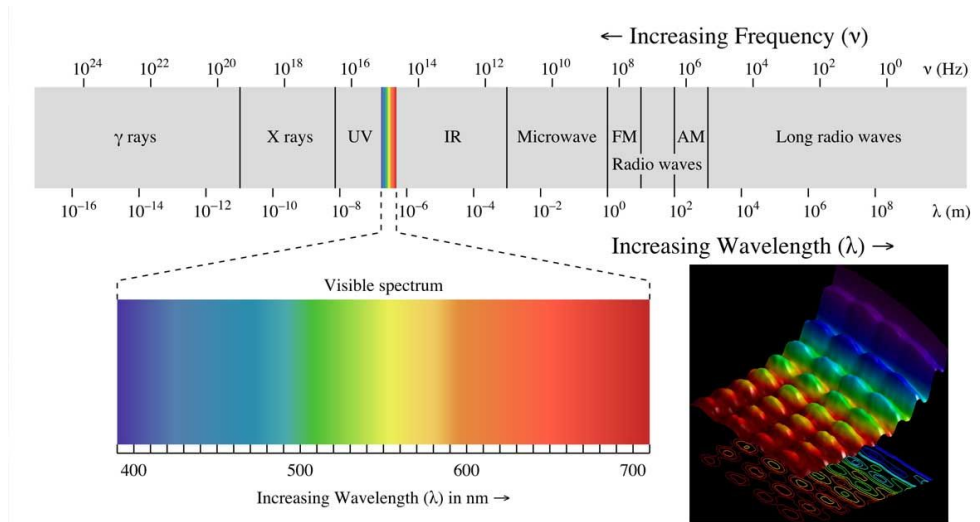


Figure 6: Visible Light Spectrum Wavelengths

2.2.2 Solar Panels

There are many varieties of solar panels but the most common types are mono and polycrystalline silicon solar panels. The difference between the two is their efficiency. With respect to silicon based solar cells, the larger the crystal the better. This is why monocrystalline cells are more efficient than their polycrystalline counterparts. However, this higher quality is reflected in the overall cost. Due to the more refined process of production, monocrystalline silicon panels are more expensive than the polycrystalline silicon variety. (Maehlum, 2018)

Photovoltaic cells collect energy from solar rays during the day. Next the energy is converted, by a solar inverter, into AC current. AC current is then distributed for practical application, in many cases to a battery or a net meter, until finally the electrical current can find a practical use powering appliances.

While there are limitless varieties of solar panels, the price of a solar panel is a reflection of both its ability to follow these steps and produce electricity, as well as the process required to produce the many solar cells a panel consists of.

2.2.3 Thin Film Solar Cells

Thin film photovoltaics were first introduced in the 1970s by researchers at the University of Delaware, but the technology has become increasingly popular in recent years [34] Thin film solar cells are advantageous over their crystalline counterparts in some applications due to the flexible, lightweight nature of the cells. Though efficiencies of thin film modules are currently less than rigid panels, 15% and 20.4% respectively, thin film cells are also less expensive to manufacture. These cells use the same concept to convert energy to electricity through the photovoltaic effect, but are produced by layering photon-absorbing materials on a flexible substrate. There are various material combinations and preparations used to construct

thin film solar cells. Some examples of thin film solar cell materials are amorphous silicon (a-Si), cadmium telluride (CdTe), and Copper indium gallium selenide (CIGS) [10]

2.2.4 Off-Grid Solar Photovoltaics

To date, off-grid photovoltaic systems have been used for camping and military operations, and by refugee or disaster relief organizations. These markets utilize portable solar PV systems in scenarios where they lack access to grid electricity. For example, off-grid systems are applicable to refugee settlements to aid in construction and maintenance of infrastructure. This applies to medical facilities, water pumping, emergency communications, and security among many others although the systems are not used for distribution to individual shelters.

2.2.4.1 General Applications

Off-grid solar voltaics are most commonly used to provide electricity for camping, the military, and off-grid homes. The characteristics of these panels vary, depending on intended application. Panels used for camping must be lightweight and portable, but do not require large amounts of energy production. These typically come in the form of a singular panel, two stiff panels that fold on top of each other, or a panel attached to a backpack, and collect sufficient energy to charge a cell phone or camera [21]. Solar lanterns and speakers are other solar-powered devices commonly used by campers [17].



Figure 7: From Left to Right: Portable Solar Charger, Solar-Powered Speaker, and Solar Lantern [17]

Military grade devices require more energy production and durability. Due to these requirements they tend to be larger and more costly. In an effort to reduce fossil fuel usage, the U.S. Marines have invested in a variety of solar products. An article published by the New York Times discusses the expenses associated with transporting and guarding fuel tanks. Though the military purchases gas at only \$1 per gallon, transportation costs per gallon can be upwards of \$400. Solar energy is a higher initial investment, but quickly outweighs these transportation costs. Some solar devices that are used by the military include foldable panels, solar tent shields, and solar chargers [24].



Figure 8: Military Grade Folding Solar Panels



Figure 9: Military Solar Energy Tent Shield

2.2.4.2 Humanitarian Applications

A benefit to off grid systems is their flexibility in design, leading to a wide variety of products. Generally, there are four types of mobile systems: all-in-one, case portable, transportable, and micro-grid.

The all-in-one solution refers to products such as a solar lamp, which has solar cells incorporated into its design that are used to generate electricity in place of a battery. This type of solution is normally on a smaller scale to the other two, as it is only feasible for small systems that do not require large amounts of electricity.



Figure 10: Solar Lamps

Case portable is an apt name for the next solution, as it refers to a product that can be transported by a single person. In this case, that includes all wiring as well as foldable solar panels. Usually this type of product is stored in a small container and removed for use during specific times of the day.



Figure 11: Case Portable Solar [6]

Transportable solutions are larger than all-in-one and case portable off-grid PV systems. The term refers to a towable product that can be used during all hours of daylight, and is often transported behind a vehicle.



Figure 12: Transportable Solar [6]

The final system is the micro-grid, the largest and most expensive of the four systems. micro-grids are PV systems that are self contained, and can be any size. Micro-grid systems are unique in the off-grid PV market because they, unlike most options, can refer to a permanent fixture. Although micro-grids are the most expensive, they also return the most electricity and can be expanded if desired. (Franceschi et al. {2}, 2014)

The Za'Atari refugee camp in Al Mafraq, Jordan has the “the largest solar plant ever built” and is a great example of humanitarian application of a microgrid. The camp provides energy for 80,000 refugees, and peaks at 12.79 megawatts of electricity entirely generated by solar cells. [12]. Za'Atari is an ideal location for such a grid due to its flat land and arid climate.



Figure 13: Za'Atari Refugee Camp Solar Grid [12]

2.2.4.3 Off-Grid Homes

A rising application of solar technology is through homes that are completely removed from “the grid,” meaning that they are self sustaining. The design of any home is specific to location due to weather and robustness required for any environment. Many homes rely on solar and wind technology for energy needs, more specifically solar panels because this style is the most efficient at converting energy to electricity.

A good example is the EcoCapsule, designed by a Slovakian company for remote places out of reach from infrastructure. This product produces a maximum of 1.35 kW of electricity, and is designed for up to two people (The EcoCapsule Team, 2017). Additionally, EcoCapsule can also harness wind and hydro energy to generate electricity. Homes such as these are becoming increasingly popular in isolated locations.



Figure 14: Eco Capsule Off-Grid Home [23]

3.0 Design

The team began the design process by identifying a problem of interest. Initially, the team wanted to develop a product that could create shade while producing solar energy as a means to reduce cooling costs. As customer interviews progressed, it was determined that displaced peoples have a great need for off-grid energy. Consequently, this product was designed for refugee populations who make up a large fraction of displaced peoples. Specifications of the design, however, could be adapted to meet the needs of the consumer. This product can be used by anyone with a need for off-grid energy.

3.1 Market Research

3.1.1 Customer Interviews

As part of the National Science Foundation's "I-CORPs" program, the team conducted thirty customer interviews. The purpose of these interviews was to identify the market that would have the greatest need for this off-grid solar product and develop a design that would be both useful and feasible. The team met with professionals from a variety of fields including solar developers, professors, employees at the Department of Energy Resources (DOER), Federal Emergency Management Agency (FEMA) officials, and campers/boy scouts. Questions were asked about energy needs in each respective field and challenges they face regarding transportation, installation, power generation, etc.

As interviews progressed it was determined that the greatest need for off-grid energy was in populations of people displaced from their homes. This includes both refugees and natural disaster victims. Key points to note from interviews about these populations are that every refugee settlement is different and electricity in camps is limited or unsafe. Low cost, transportability, simple setup, and low maintenance should be prioritized in the design. The value of this product to consumers is green energy that is easily transported, deployed, and operated at low cost.

3.1.2 Disaster Relief Workshop

The Field Innovation Team (FIT), led by Desi Matel-Anderson, invited the MQP team to Washington D.C. to participate in their "Do Tank." In attendance at the event were individuals of varied backgrounds ranging from Executives of FEMA to employees of the home restoration business Paul Davis Co..

The Do Tank is designed to find new and creative solutions to real world disasters. It entails a three step process that consists of identifying the who, the what, and the how. "The who" refers to those affected by the disaster and their specific needs. Then participants brainstormed solutions to satisfy needs of the disaster victims during "the what" portion of the Do Tank. Finally, everyone formed groups during "the how" portion to combine ideas to create a

new and unique solution. The Do Tank in Washington D.C. was held to solve a snowstorm scenario.

For the purposes of this project, the Do Tank provided insight into how different organizations analyze disaster relief solutions. For example Kim Kadesch, the Director of the Office of National Capital Region Coordination at FEMA, insisted that the first step to be taken is establish transit systems so that emergency health services can be reestablished. Another individual named John Ingargiola, an engineer who works for FEMA, focused more on what can be done to improve homeowner disaster preparation. All these perspectives are taken into account during brainstorming and then refined during a group session until there is a final solution.

FIT instructed participants to ignore the logistics of any solution up until the final group session. At this point, logistics played a large part in the solution. From the results we witnessed, an underlining logistic factor is transportation. There must be a regulated size and material weight that allows for relief organizations to quickly mobilize and deploy. There was also great emphasis not on the size of a package being transported, but on the area of livable space provided by a temporary shelter. This is because involved relief organizations must be prepared to provide every family or citizen with equal space and amenities, or risk inducing a frenzy for supplies.

FIT employs the Do Tank to find innovative solutions to disaster scenarios, and is successful because this method combines a wide variety of perspectives and analyses prior to generating solutions. In addition to our participation in the Do Tank, FIT agreed to evaluate the final product of this MQP, and will provide their thoughts on how it can be improved and deployed in disaster relief.



Figure 15: Photo from DO Tank at HSEMA⁴

3.2 Design Criteria

Background and market research were used to establish design criteria that would best satisfy consumer needs. These criteria include: electrical production, transportability, rapid deployment, and low cost.

3.2.1 Electrical Production

The first criteria considered was electrical production. With respect to solar energy, electrical production is a function of size and orientation when exposed to the same sunlight. To determine what size solar panel is needed, the energy requirements of the end user were taken into consideration. Currently, many refugees do not have any access to electricity, so electrical requirements were made based on basic functions such as cooking or lighting as shown in Table 1.

Table 1. Energy Requirements Per 60 Minutes

Energy Requirements per 60 minutes				
	Washer	Iphone	Boiling (1 L from 20C)	Light Bulb (60W)
Energy Requirement (J)	1,116,000	36,000	330,694	216,000

3.2.2 Transportability

Transportability of a product is mainly governed by size, weight, and geometry. The amount of products that can be transported is limited by the size of the device. The more compact a design is, the more devices can fit inside a cargo truck. This in turn, will minimize transportation costs. The device should also be light enough that no more than two people are required to lift it. The National Institute for Occupational Safety and Health (NIOSH) has established a safe weight lifting limit of 51 pounds per person [39]. Weight can be controlled by both size and material selection. Lastly, geometry plays a role transportability of a product. Though boxes stack better for storage, cylindrical shapes can be rolled for easier loading.

3.2.3 Deployment

One drawback to traditional solar panels is installation time. The average residential solar installation process takes three months, but can even take up to six months [28]. For people displaced from their homes, that is an extensive amount of time to spend without electricity. Solar developers are also required to safely install residential panels. The chosen design must be capable of rapid deployment that does not require an understanding of electrical systems to set up.

3.2.4 Cost

The cost benefits of solar energy are most apparent over long term analyses. Though the capital cost may be higher than that of fossil fuel energy sources, solar energy does not incur operating costs. This type of investment is particularly intuitive in the case of refugee camps. Organizations, such as UNHCR, that provide resources to refugees have pre-established budgets. Solar energy would allow UNHCR to account for one upfront cost and eliminate variable operating costs. The Za'Atari Camp is a prime example of the benefits of solar energy with respect to cost. The Government of Germany invested \$17.5 million into construction of the solar field, but estimates \$5.5 million in annual savings. (Hashmen, 2017) Cost is also taken into consideration for design based on material consumption and manufacturability.

3.3 Preliminary Designs

Preliminary designs were made throughout the research process and modeled in SolidWorks. All designs implement solar technology, but functionality and appearance varies greatly. The design intent and target market shifted during the research process, so the designs progressed accordingly. Once design criteria was established, the team was able to select a design which best solved the problems being addressed in this project.

The rotating canopy preliminary design was created first. This design was made with the intent to provide electricity as well as shade. The design incorporated solar panels attached to a flat platform along the center beam as shown in Figure 16. In addition to solar panels, the system would be able to rotate around the center beam to account for the sun's position in the sky, and to maximize solar absorption. This design could effectively produce shade and electricity, however it was not a significant innovation from existing solar panels. It would consume as much space as traditional panels and would not be any easier to transport.

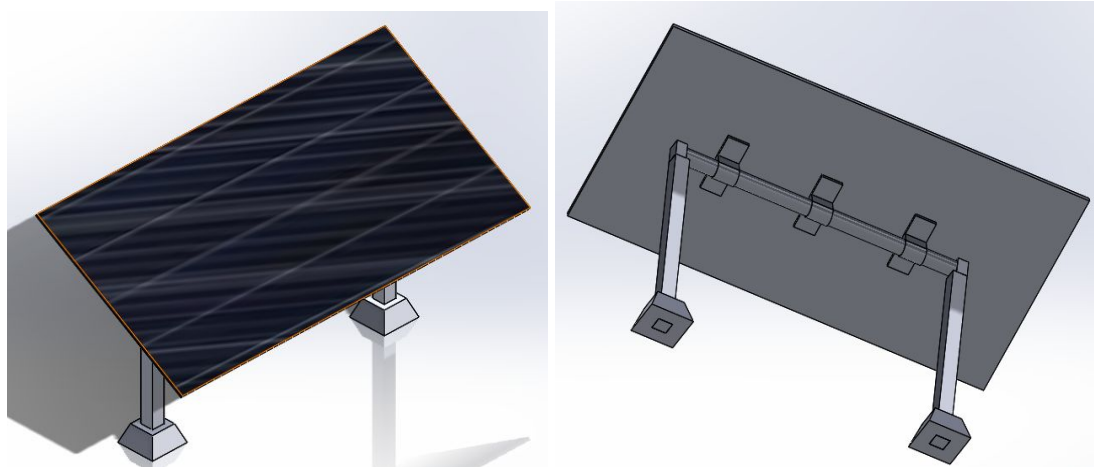


Figure 16: Rotating Canopy

The following designs are similar conceptually. These designs also served the purpose of creating shade and providing electricity. The structure is a stand-alone foldable awning with thin

film solar cells attached to the canvas. The legs would unfold and lock into place for ease of transportation and set up. A user-controlled crank mechanism would extend and retract the canvas and solar cells. There are two variants of this design: one with a vertical support and one with a diagonal support. If the awning design was chosen, it would have been assessed to select the structural variation that maximized sturdiness. The awning design allowed more usable space below the structure, but still would consume space that may not be available. It would be relatively easy to set up and transport, but ultimately was eliminated as it was outperformed by a future design in these categories.

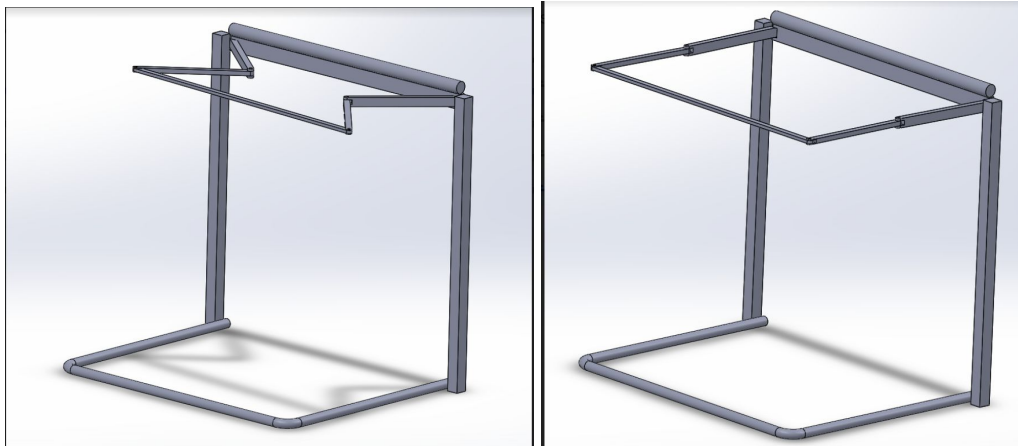


Figure 17: Awning Design 1

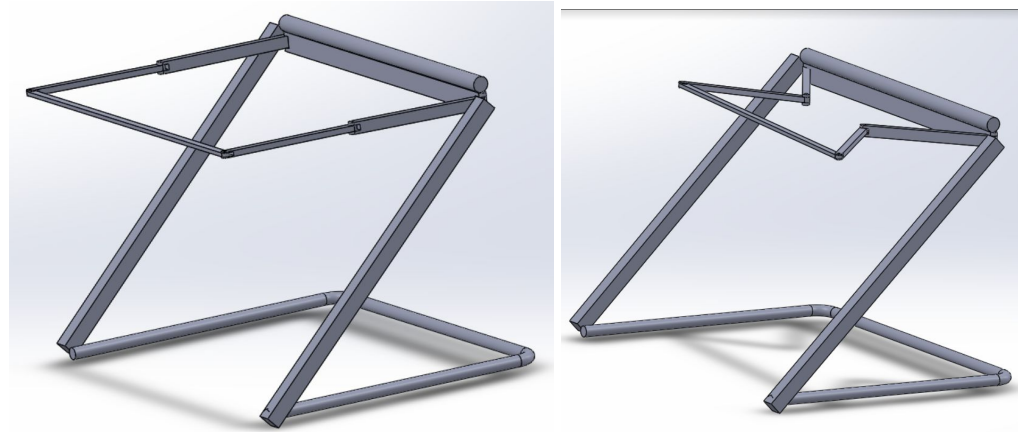


Figure 18: Awning Design 2

The next of the preliminary designs was a PV system designed to provide shade over a home to reduce cooling costs while supplementing solar energy to the home. The structure would stand roughly 20 feet high, the height of a two story home, and resembles a tree. The solar cells would be placed along strips of reinforced fabric to resemble a palm frond. The system uses a number of palm fronds arranged on top of a hollow pole to provide support and act as a storage container. The palm fronds would be deployed using a pulley mechanism controlled by the user. The fronds hang outwards to provide shade and collect energy. This system was eliminated

because the design is less applicable in humanitarian endeavors. Additionally, it may not provide ample shade or energy production.

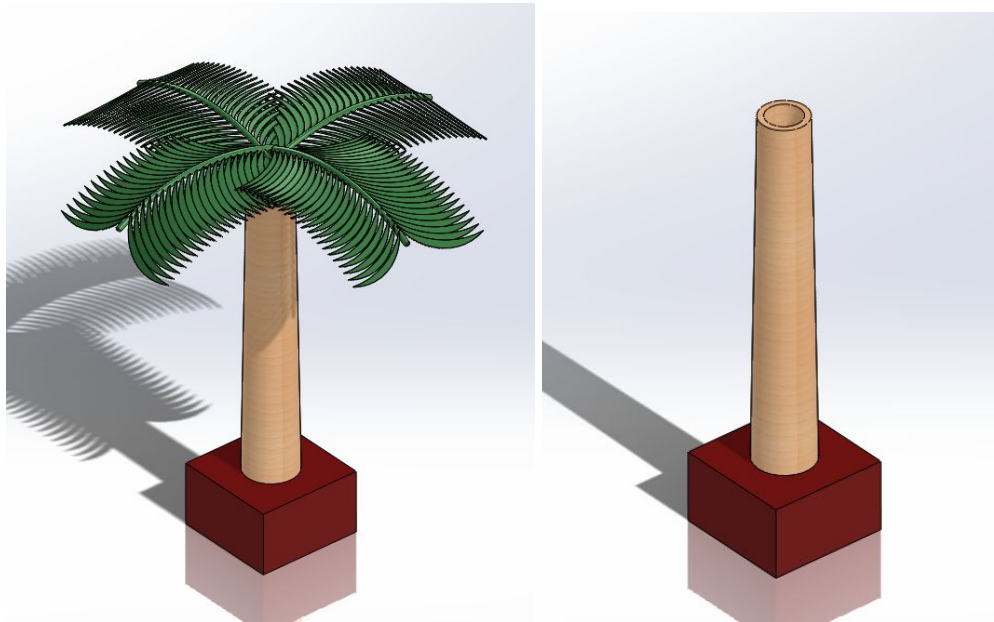


Figure 19: Palmbrella Energy & Shade System

One proposed design was made with the intention of collecting rainwater and producing solar electricity. Solar panels would be arranged in an inverted umbrella shape. This shape would form a funnel to direct water down a tube. Within the tube, there would be a filter to remove contaminants from the water. The water would proceed down the tube where it would be stored in a tank. There would be a pumping mechanism within the tank so the water could be used at will. This design (shown below) was ultimately eliminated due to limited transportability and prioritization of electricity production over water collection.



Figure 20: Solar Energy Water Collector

The next preliminary design was a tent addition designed for center pole tents. Thin film solar cells would be attached to a lightweight fabric cut into a conical design such that it would wrap around the roof of a center pole tent. This proposed style would be useful in humanitarian application because it saves space in the communities. Additionally, this design was also appealing due to its simplicity, The addition would be attached to the tent structure and supply electricity to a battery, requiring some maintenance of the battery and solar cells to ensure efficient electricity production. Research showed that refugees in the target region live in “UNHCR Family Tents for Hot Climates,” which is not a center pole tent [32]. As a result of this research, the design was determined to be unfeasible in this application and other possible iterations were investigated.

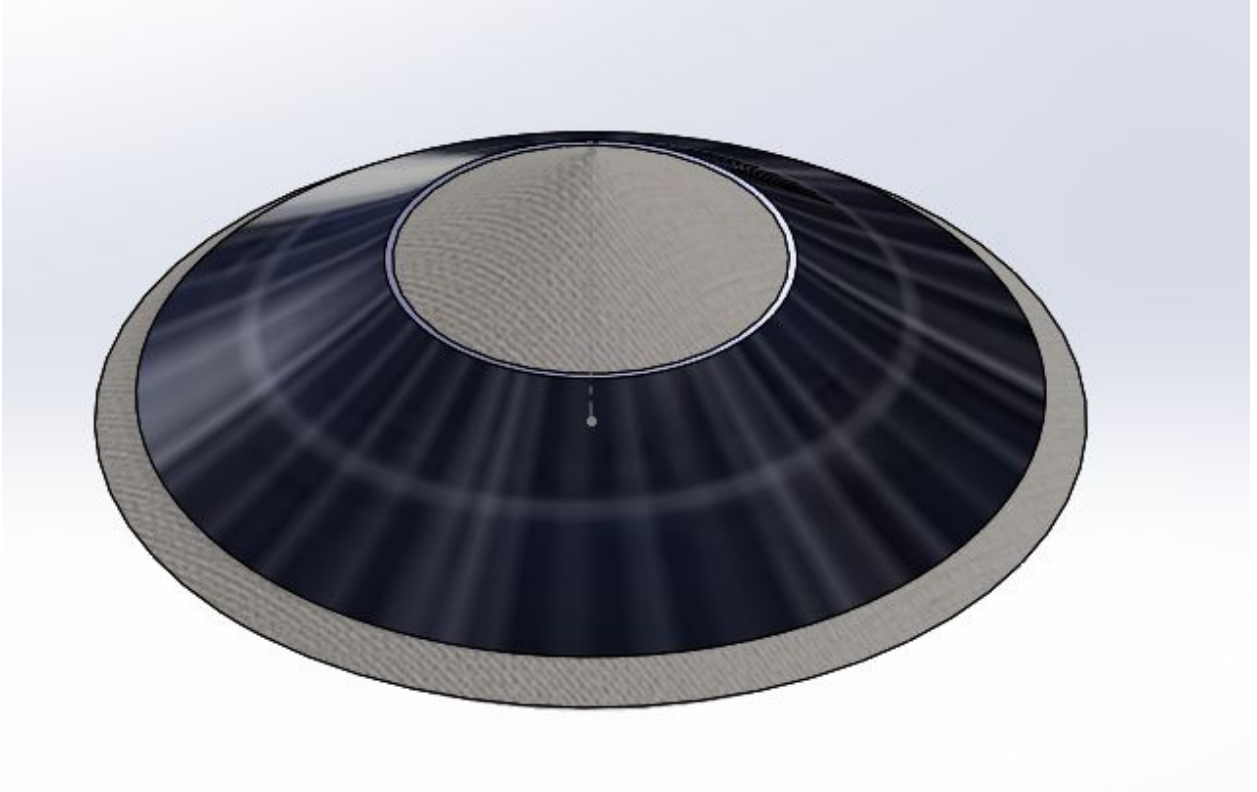


Figure 21: Center Pole Tent Addition

The final proposed design is an addition to a pre-existing tent. This design utilizes the concept of a tent fly to also produce electricity from sunlight. Tent flies are fabric coverings commonly used to provide shade and protect the tent from rain. The differentiating factor lies in the roller spring mechanism designed for ease of deployment. The fly is housed in a spring-loaded cylindrical container and can be extended and retracted by pulling the end of the fly. The fly is then fixed to the ground using guy ropes or stakes through grommets on the fly's end. This design would effectively produce electricity without using additional space. It is compact when stored in its container and, therefore, easy to transport.



Figure 22: SolidWorks Model of SolFly Design with Four Solar Panels

3.3 Final Design

3.3.1 Design Constraints

This project was designed using the “Family Tent for Hot Climate” protocol as parameters. The protocol document for each climate specifies the design characteristics of each tent such as material composition, tensile strength and water vapor permeability. In addition to characteristics, the document contains dimensions of individual parts as well as instructions for assembly and storage [32]. The constraints of this project are closely aligned with the “Family Tent for Hot Climate” protocol because the new component is designed as an attachment for tents currently in use. Shown below is a figure of the tent from this protocol and some associated dimensions.

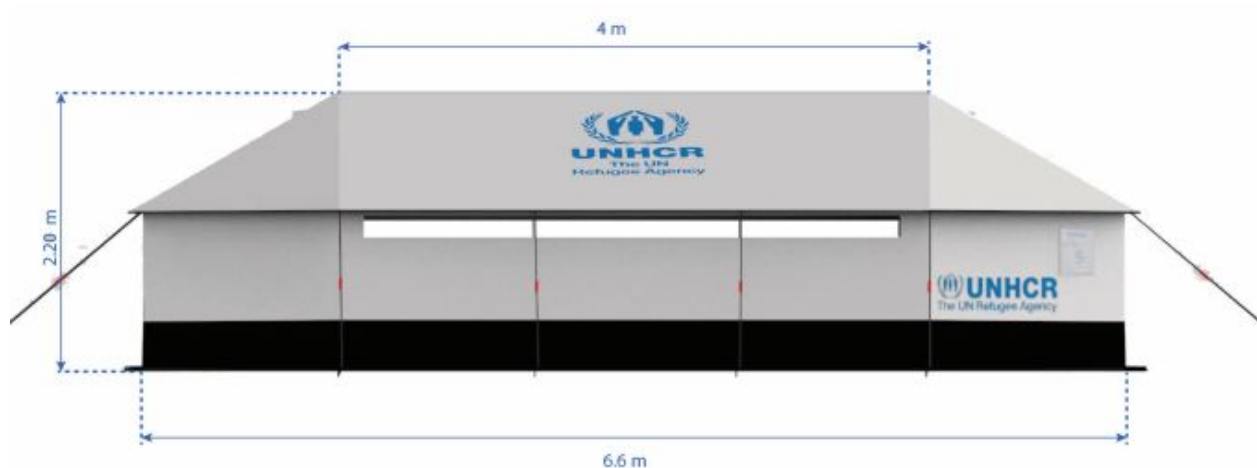


Figure 23: Side View of UNHCR “Family Tent for Hot Climate” [32]

This tent is deployed in countless refugee camps found in hot climate regions globally. A global horizontal irradiance (GHI) map (shown below) can be observed in order to identify which of these camps would be best fit for implementation of solar energy. GHI indicates the amount of solar radiation received by a horizontal surface. Locations with overlap of high refugee populations and high GHI, approximately 6.6 kWh/m^2 , include Jordan and Namibia [27]. These regions are selected as potential candidates for use of SolFly.

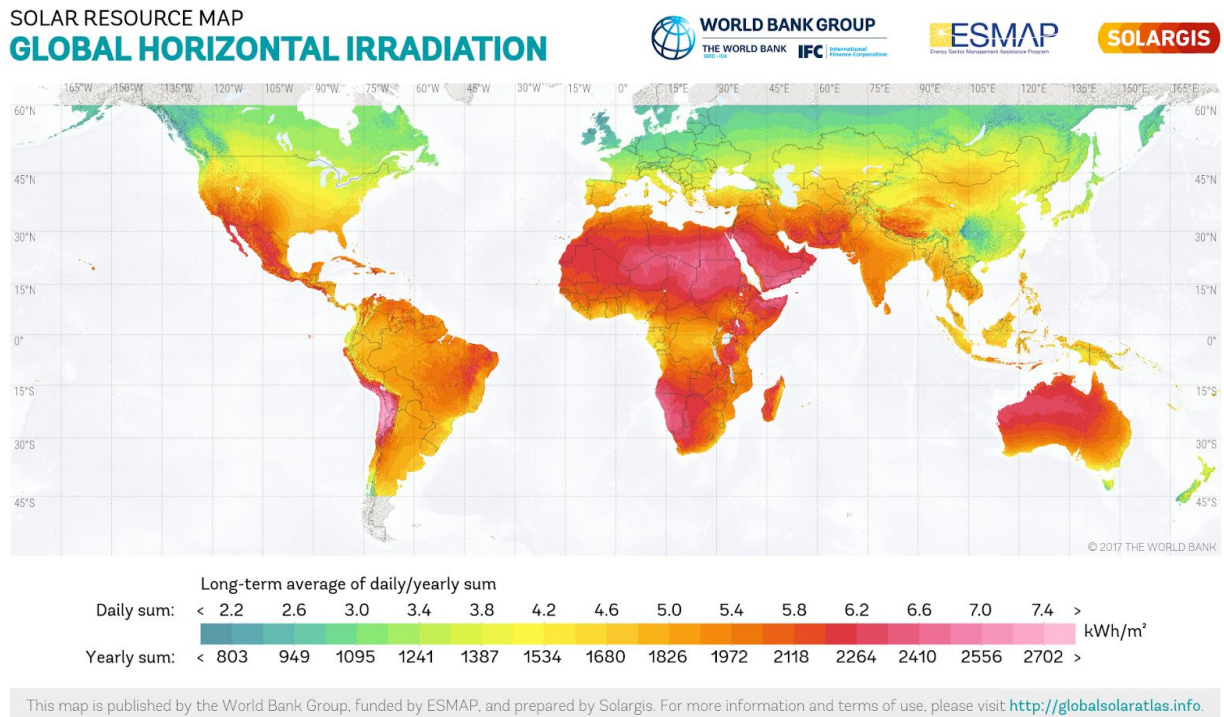


Figure 24: Solar Resource Map: Global Horizontal Irradiation [27]

3.3.2 Features

The final design has three major components: the PV system, tent fly, and spring mechanism. The PV system consists of a thin film solar cell array that is wired to an electrical outlet box and a storage battery. The electrical outlet box is set up inside the tent, to power indoor lights and other devices. The solar array is stitched onto the fly. The tent fly serves the dual purpose of a base for the solar array while protecting the tent from exposure to the elements. The fly is housed in a container with the spring mechanism. When the fly is extended, spring torsion is built up. The fly clicks into place using ratchet and pawl mechanics. When lightly tugged, the fly fully retracts into the housing for quick storage. The final design is branded as “SolFly”

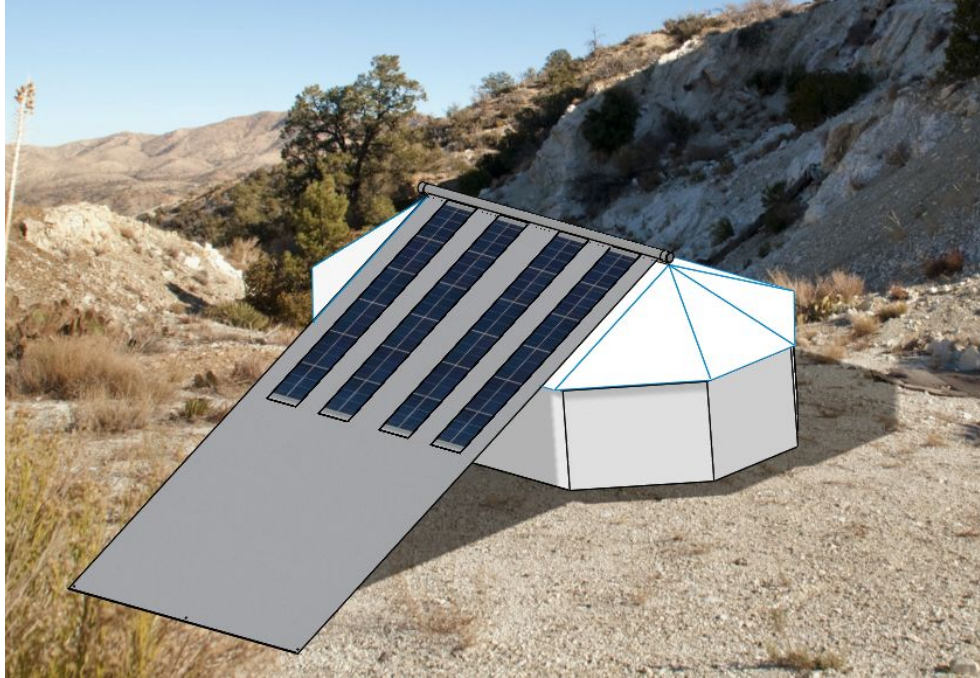


Figure 25: Concept SolidWorks Model of One SolFly on UNHCR “Family Tent for Hot Climate”

3.3.3 Materials Selection

The solar array and component materials were selected by using design matrices to compare viable options.

3.3.2.1 Solar Cell Selection

In order to select the best solar technology for the design, a variety of thin film cells were compared in a design matrix. Factors for comparison in the design matrix were wattage per area, weight per area, cost per area, and flexibility. Each factor was weighted according to importance.

Table 2. Product specifications for each of the solar panels

Number	Length (in)	Width (in)	Area (in ²)	Watts (W)	Weight (lbs)	Cost (\$)
1	45.87	22.4	1027.488	100	4.4	250
2	46.8	21	982.8	100	4.1	169
3	61.8	36.2	2237.16	300	N/A	478.99
4	216	15.5	3348	136	17	194
5	138.2	19.05	2632.71	100	7.06	100
6	20.5	13	266.5	30	1.32	58

Table 3. Solar Cell Design Traits with respect to Area

Number	Watts/in ²	Weight/in ²	Cost/in ²
1	0.0973	0.0043	0.2433
2	0.1018	0.0042	0.1720
3	0.1341	N/A	0.2141
4	0.0406	0.0051	0.0579
5	0.0380	0.0027	0.0380
6	0.1126	0.0050	0.2176

Table 4. Solar Cell Design Matrix

Number	Wattage (W)	Weight (lb/in ²)	Cost (\$/in ²)	Flexibility	Total
1	3	4	1	3	11
2	4	4	4	1	13
3	6	0	3	1	10
4	1	2	5	4	12
5	1	6	6	6	19
6	5	2	2	3	12

It was determined that option number five best fit the design criteria for this project. This option is a thin film a-Si solar cell manufactured by F-WAVE (shown below). Besides the factors for consideration included in the matrix, F-WAVE cells show a greater increase in efficiency when operated at high temperatures than their crystalline counterparts. This is due to the annealing effect which “causes hydrogen atoms to bond returning the power output of an amorphous solar cell to its initial value.” [7] The figure below shows power generation over time of an a-Si F-WAVE solar cell compared to a crystalline solar cell. This is advantageous in the case that SolFly will be employed in hot climate regions such as Africa or the middle east where temperatures can be at least 80° year round.

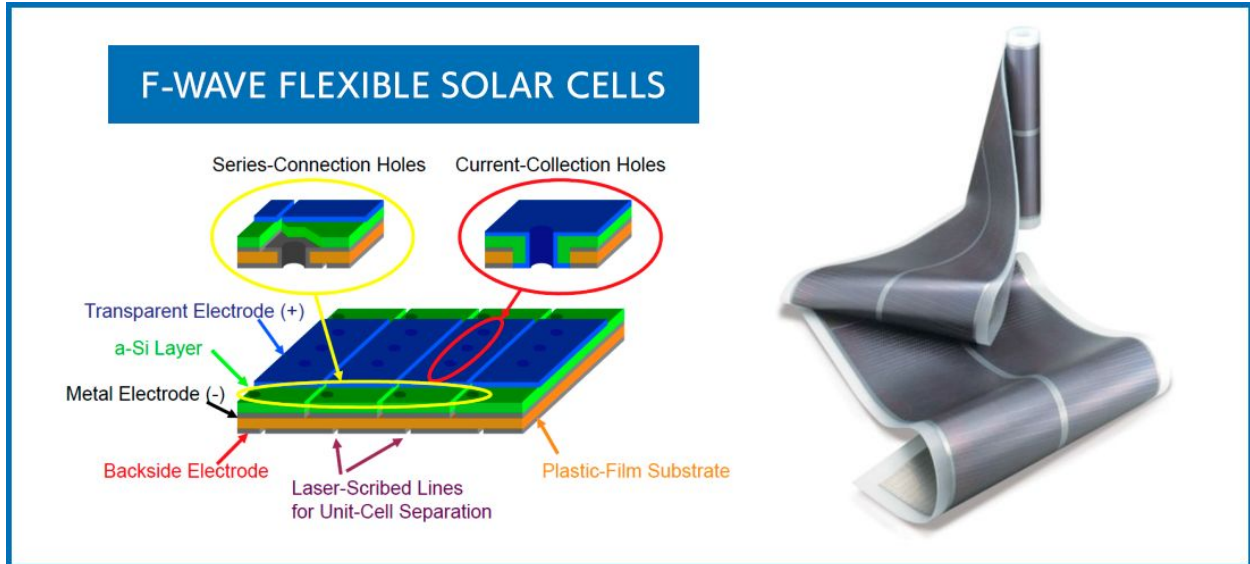


Figure 26: F-WAVE Flexible Solar Cells Diagram [7]

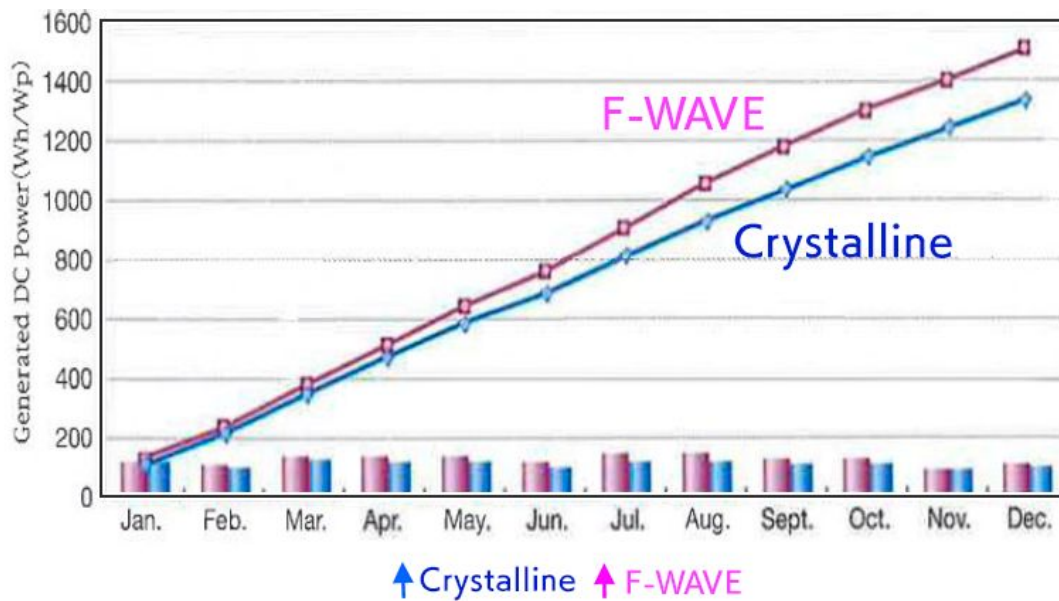


Figure 27: Power Generation over time of F-WAVE Flexible Solar Cell Compared to Crystalline Solar Cell [7]

3.3.2.2 Tent Fly Material Selection

The tent fly material was selected from the two fabrics most commonly used to make rain flies for tents: nylon and polyester. Both materials are lightweight and waterproof. It is important that nylon and polyester used for tent flies be treated or coated to prevent rips. Ultimately, nylon was selected because it is not heat conductive and is resistant to ultraviolet light. More specifically, Nylon 6,6 is used for tent applications because it is stronger and stretches less than Nylon 6. (Hayes, 2013) The ripstop nylon selected for this purpose is polyurethane (PU) coated for increased water resistance and has a 2000mm hydrostatic head rating. It is treated with UV inhibitor to further protect from sunlight and FR coating for

fire retardancy [18]. These properties combined make nylon the most suitable material for the solar energy tent fly. Further discussion and testing of the nylon fly can be found in section 5.3.

3.3.2.3 Housing Material Selection

The housing material was selected from a variety of materials typically used for outdoor furniture. These options included: aluminum, plastics, steel, wood, and wrought iron. Because each material has very different properties, they were compared by pros and cons rather than a design matrix.

Table 5. Comparison of Housing Material Options

Material	Pros	Cons
Aluminum	Lightweight Durable Low Maintenance Inexpensive	Hot in sunlight
Plastic	Lightweight Low Maintenance Inexpensive Easy to manufacture	Less sturdy
Steel	Sturdy Durable	Heavy Hot in sunlight
Wood	Sturdy Non-heat absorbing	Expensive High Maintenance
Wrought Iron	Sturdy Durable Weather Resistant	Very heavy

It was determined that plastic would be the most suitable material for this application. Plastic is lightweight, low maintenance, inexpensive, and manufacturable. Aluminum has comparable properties, however materials that get hot in sunlight were eliminated. This device will face prolonged sun exposure in hot climates and could pose a danger to users if temperatures are too high. The heavy materials were also eliminated, to avoid unnecessary burden of weight on the tent frame that could result in structural failure. Though plastic is less sturdy than the other options, it is not a limiting factor for this purpose. The housing will not be subjected to excessive strain [35].

The material was then further narrowed from an array of plastics used for outdoor applications. Some potential outdoor applications of plastics are outdoor glazing, outdoor signs,

and wood replacements. The latter is the most fitting category for this application. High density polyethylene (HDPE), ultra high molecular weight polyethylene (UHMW-PE), and expanded polyvinyl chloride (PVC) are plastics commonly used as wood replacements. Of these materials, HDPE has the most desirable characteristics being durable, wear resistant, easy to fabricate, and easy to clean³. HDPE was chosen as the material for the housing and similar parts.

3.3.4 Modeling

All components and assemblies were modeled in SolidWorks. Engineering drawings with appropriate dimensions are shown below. Design is intended for manual assembly and all parts are assembled in one direction to minimize production time.

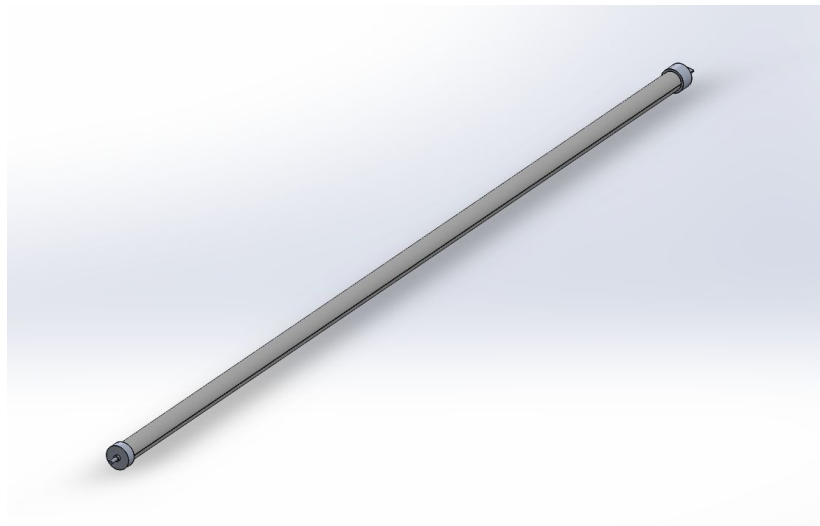


Figure 28: Spring Mechanism Assembly Model in SolidWorks

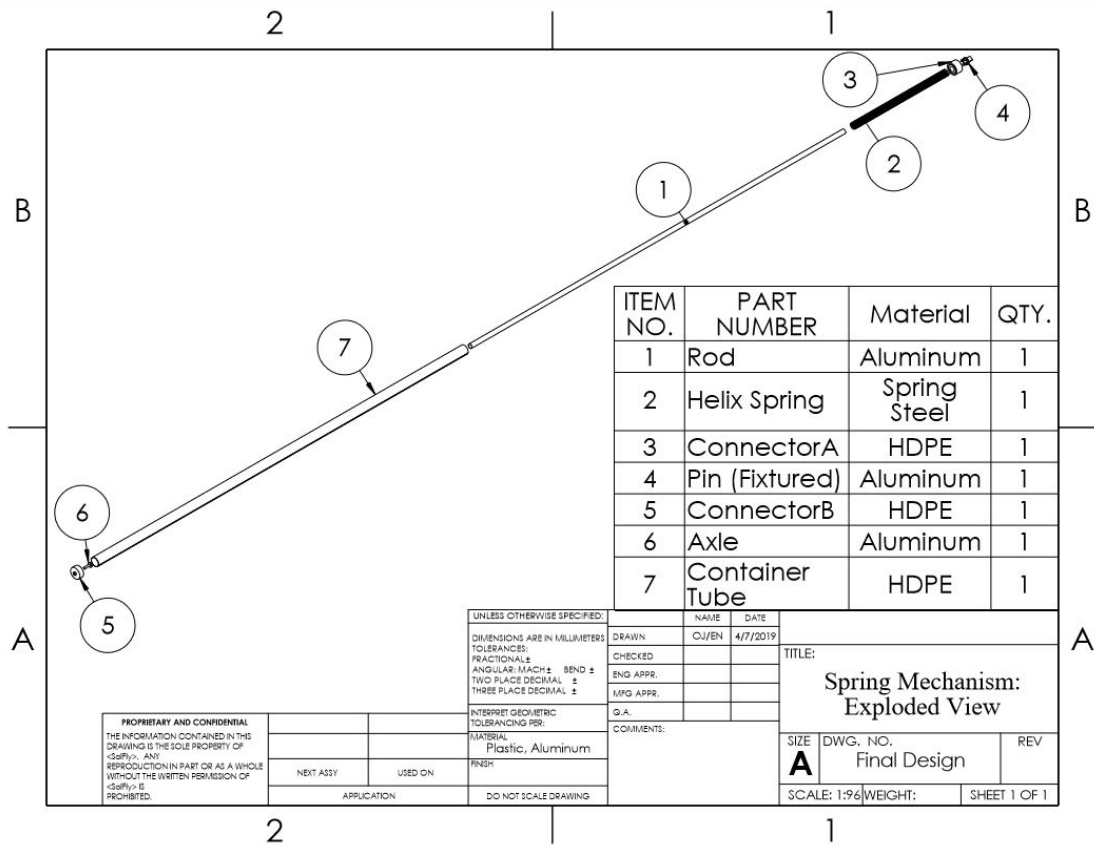


Figure 29: Drawing of Spring Mechanism Subassembly: Exploded View with Bill of Materials

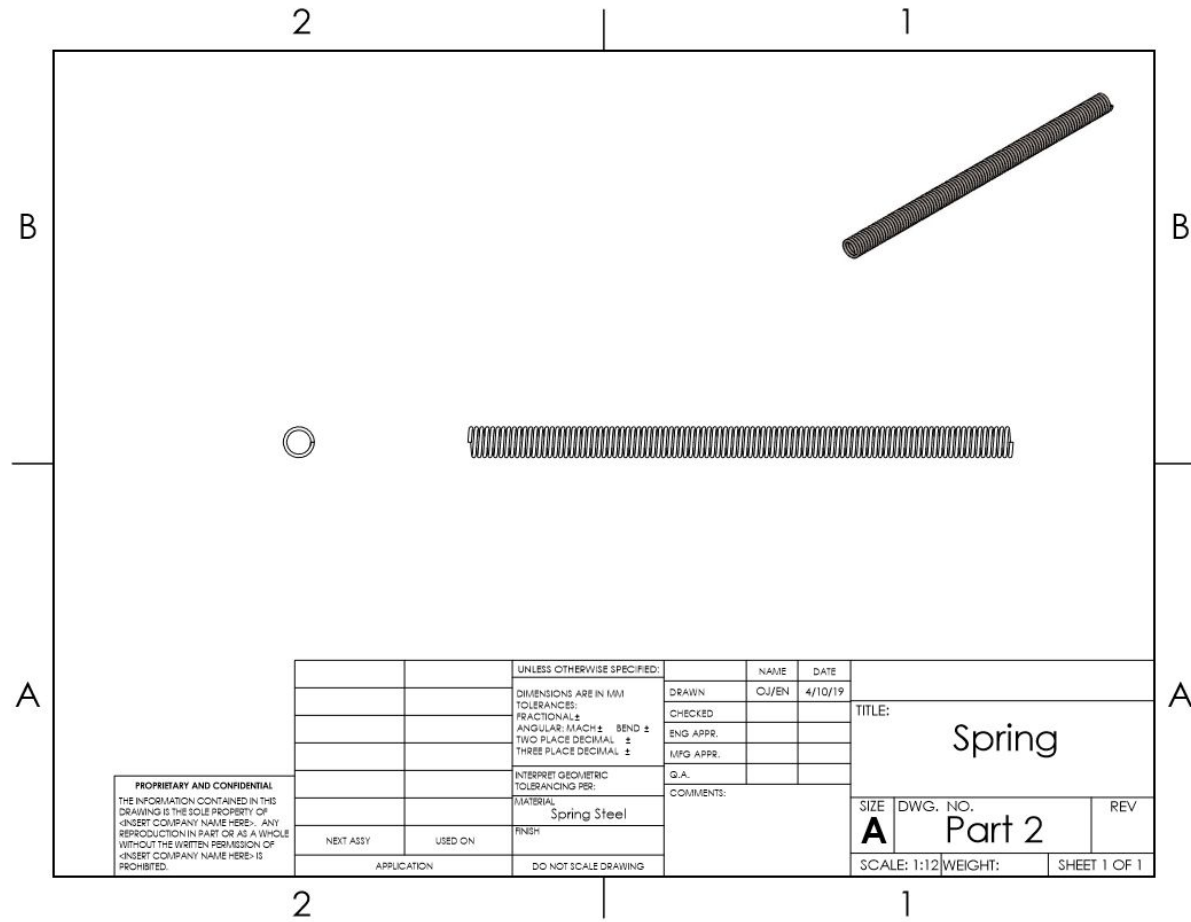


Figure 31: Drawing of Helix Spring

The spring surrounding the rod is the driving mechanical force of SolFly. For this reason, spring dimensions are dependent on desired torsional spring constant. The spring constant requirement increases with the overall weight of the tent fly and solar panels. Calculations for this parameter can be found in the analysis section. The spring is made of spring steel.

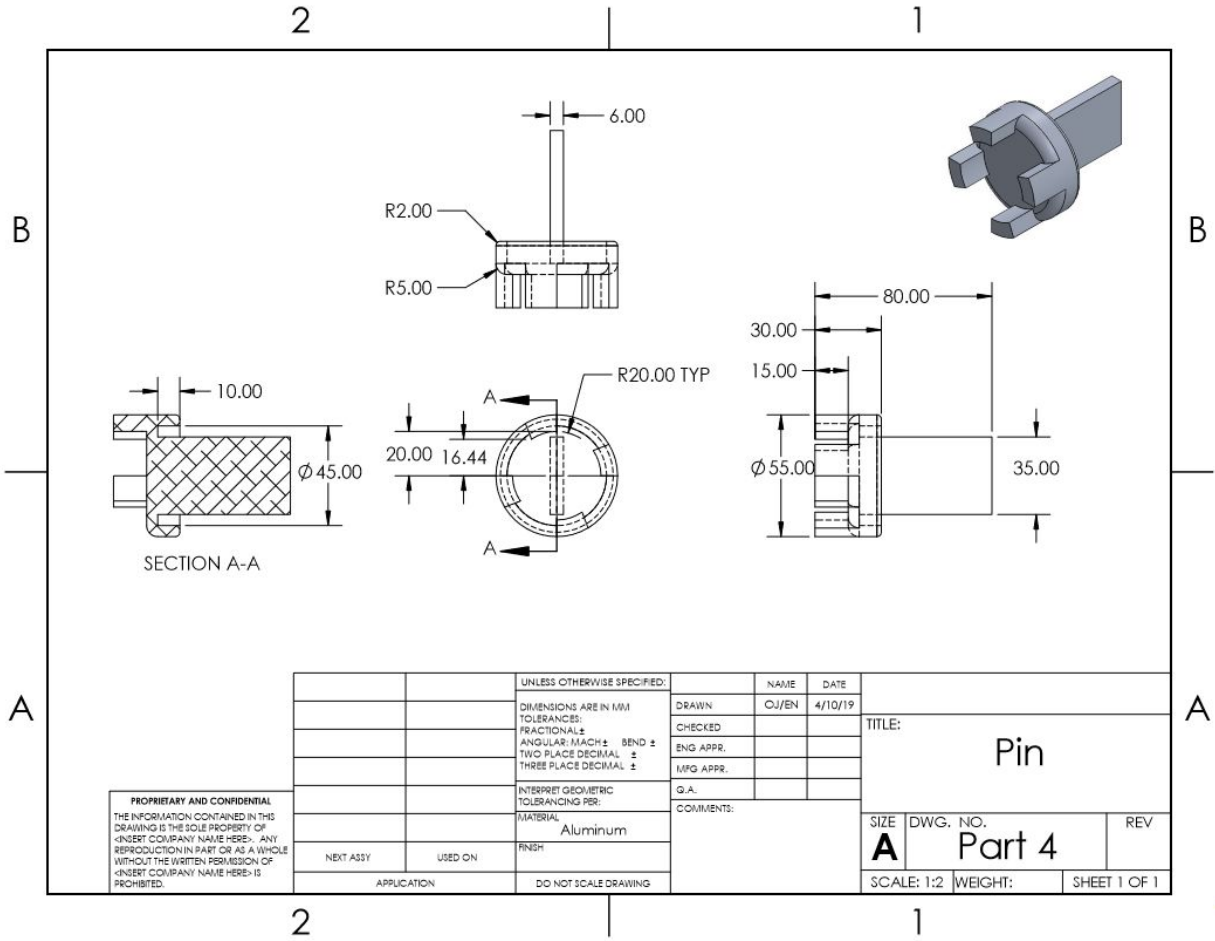


Figure 33: Drawing of Pin

The pin connects to both the rod and connector A. It serves as the ratchet for the pawl. The pin is inserted into the cap which remains stationary while the spring rotates.

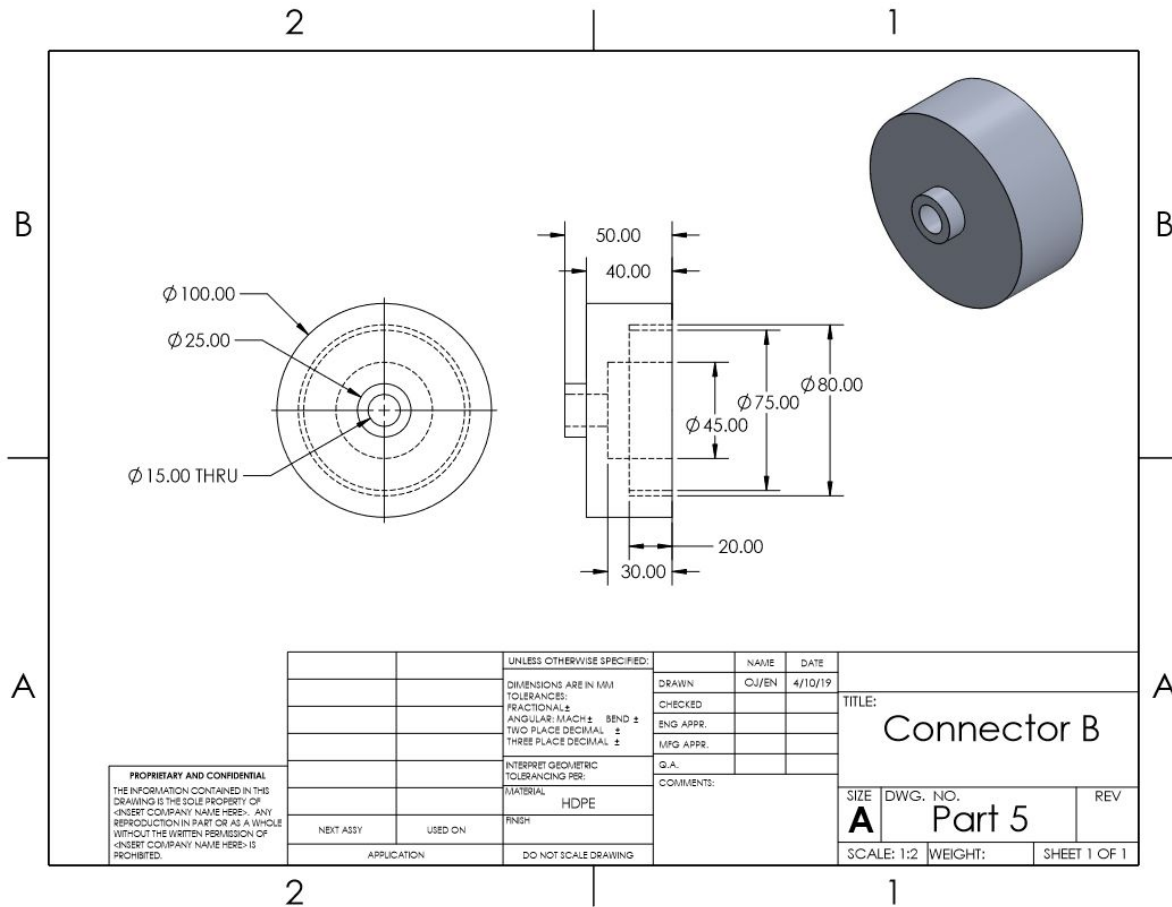


Figure 34: Drawing of Connector B

Connector B also attaches the spring mechanism to the inside of the housing. The rod is inserted as well as the spring container. The difference between the two connectors is connector B houses the axle rather than the pin.

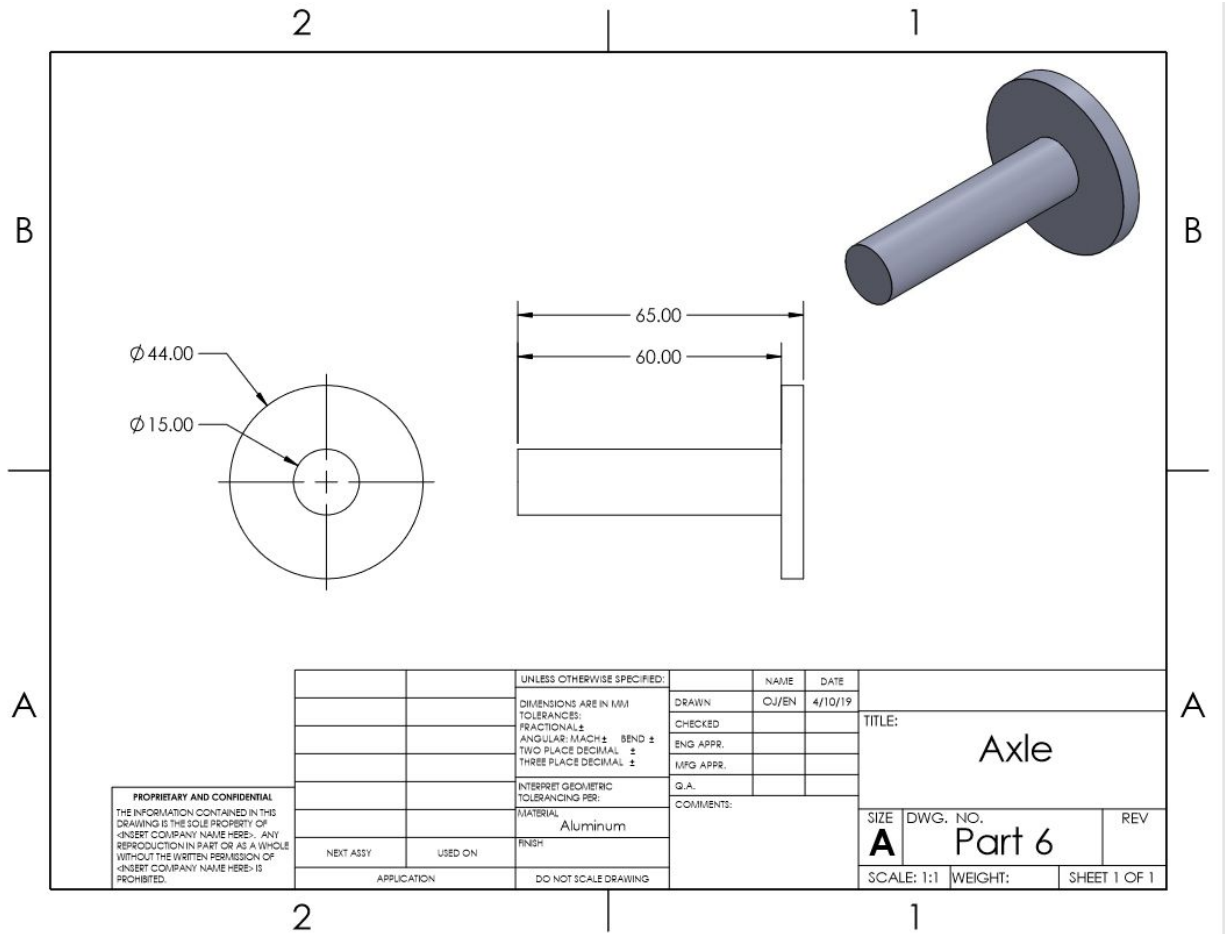


Figure 35: Drawing of Axle

The axle is inserted into connector B and the rod is adhered to the opposite side. The axle extends through connector B and is inserted into cap 2, where it can rotate freely.

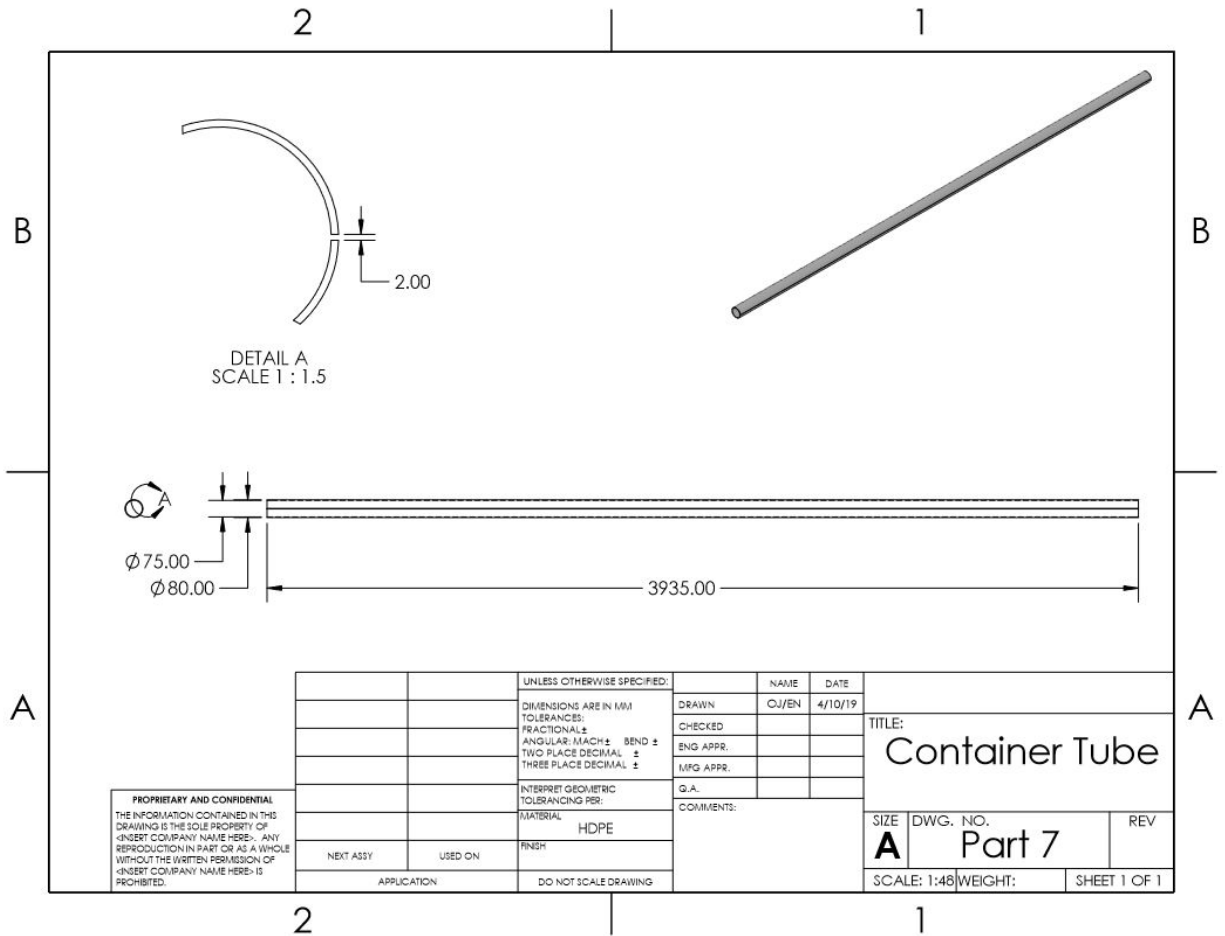


Figure 36: Drawing of Container Tube

The tube contains all components of the spring and is held together on either end by the connector parts. The end of the fly, which contains a rod to hold it in place, is also inserted into the slit of the container tube so that it rotates with the spring

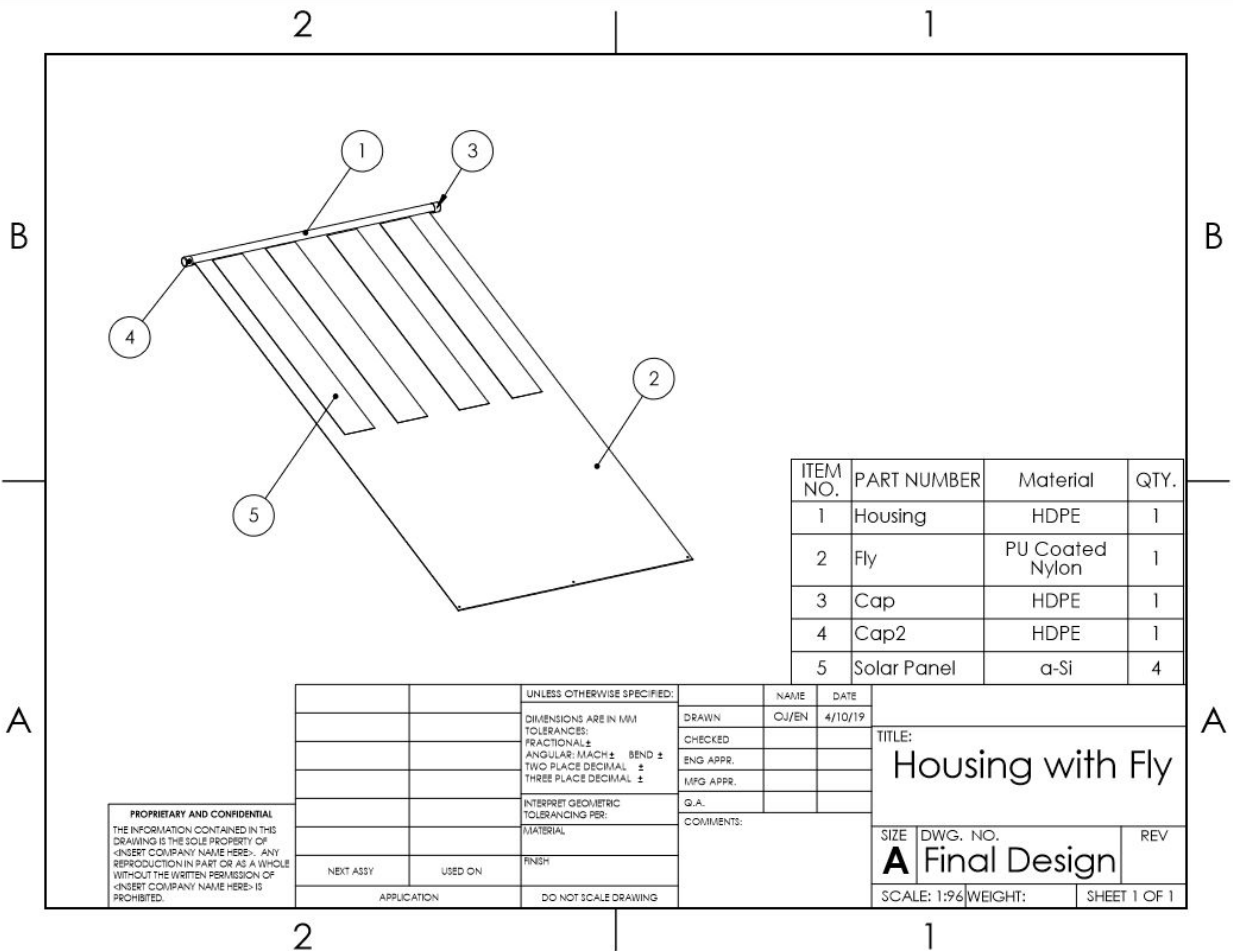


Figure 37: Drawing of Housing with Fly Subassembly with Bill of Materials

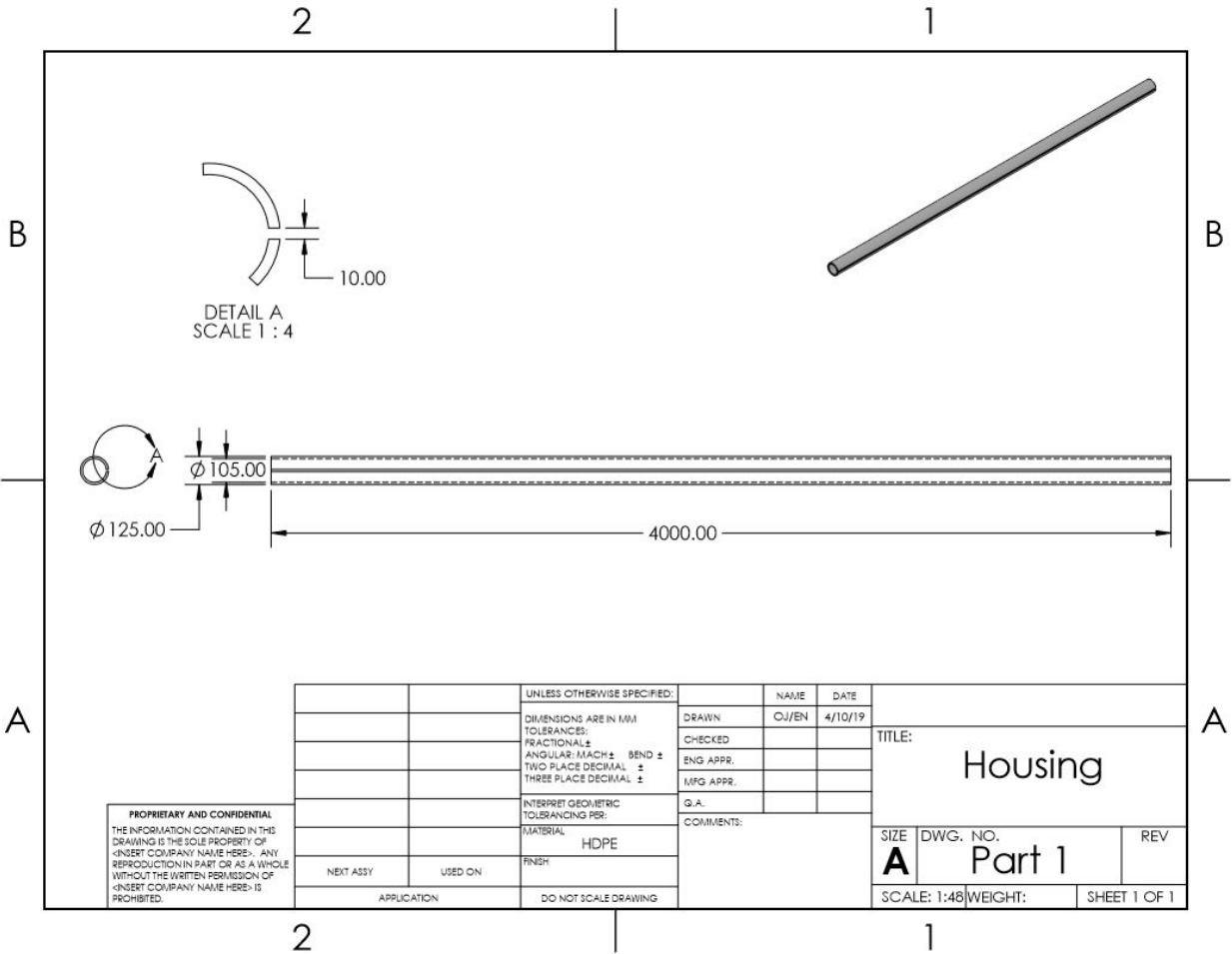


Figure 38: Drawing of Housing

The housing contains the spring mechanism and the fly rolls inside of the tube. This protects the device and makes it easy to store and transport. The electrical wiring is also stored in the housing.

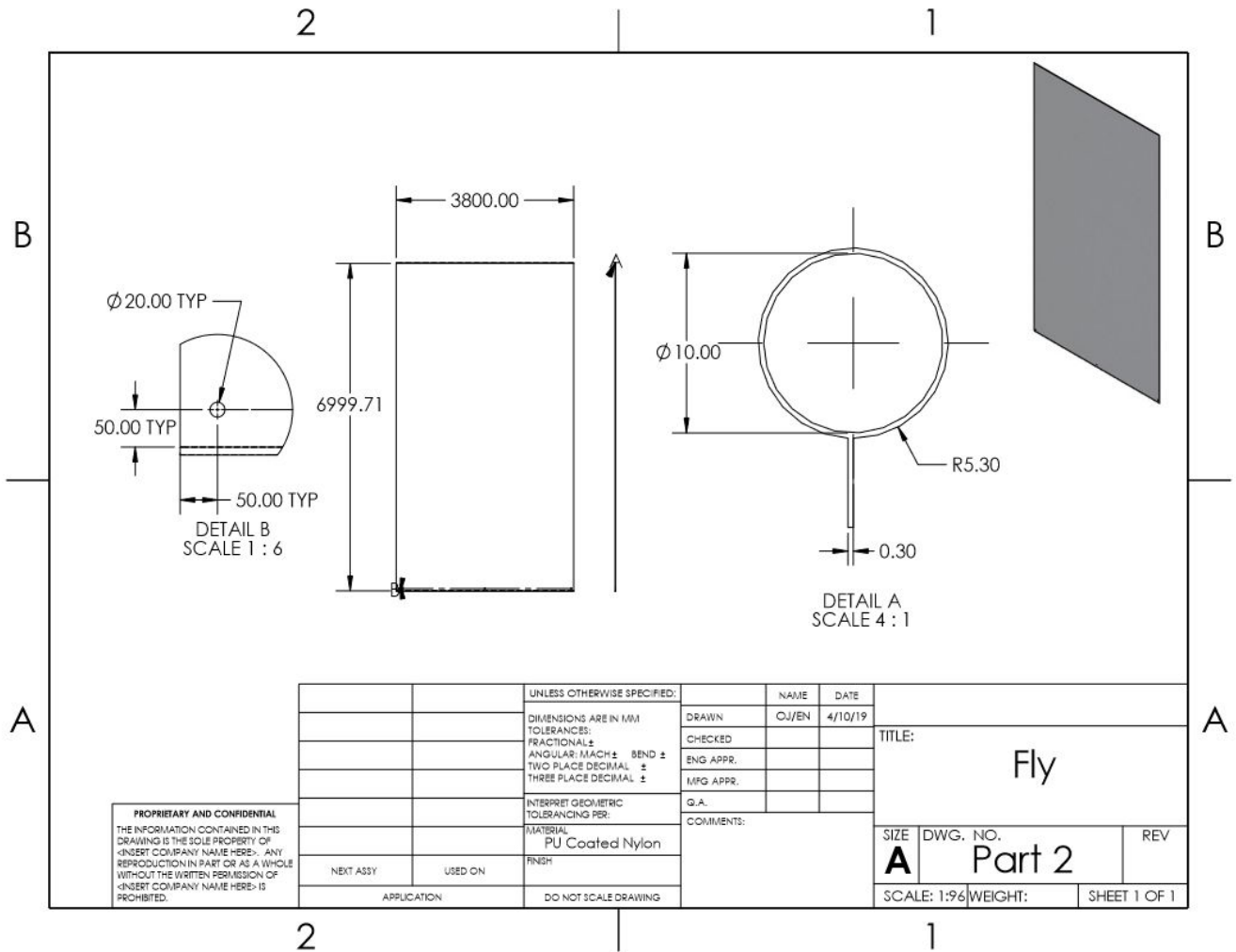


Figure 39: Drawing of Fly

The fly was designed to extend over the tent so that it does not touch it, and serves as a protective covering. A loop, shown in Detail A, is sewn on one end to insert a rod. The rod holds the fly into the spring mechanism. There are holes for grommets and stakes in the corners and center of the bottom of the fly. Dimensions of holes are indicated in Detail B of Figure 39.

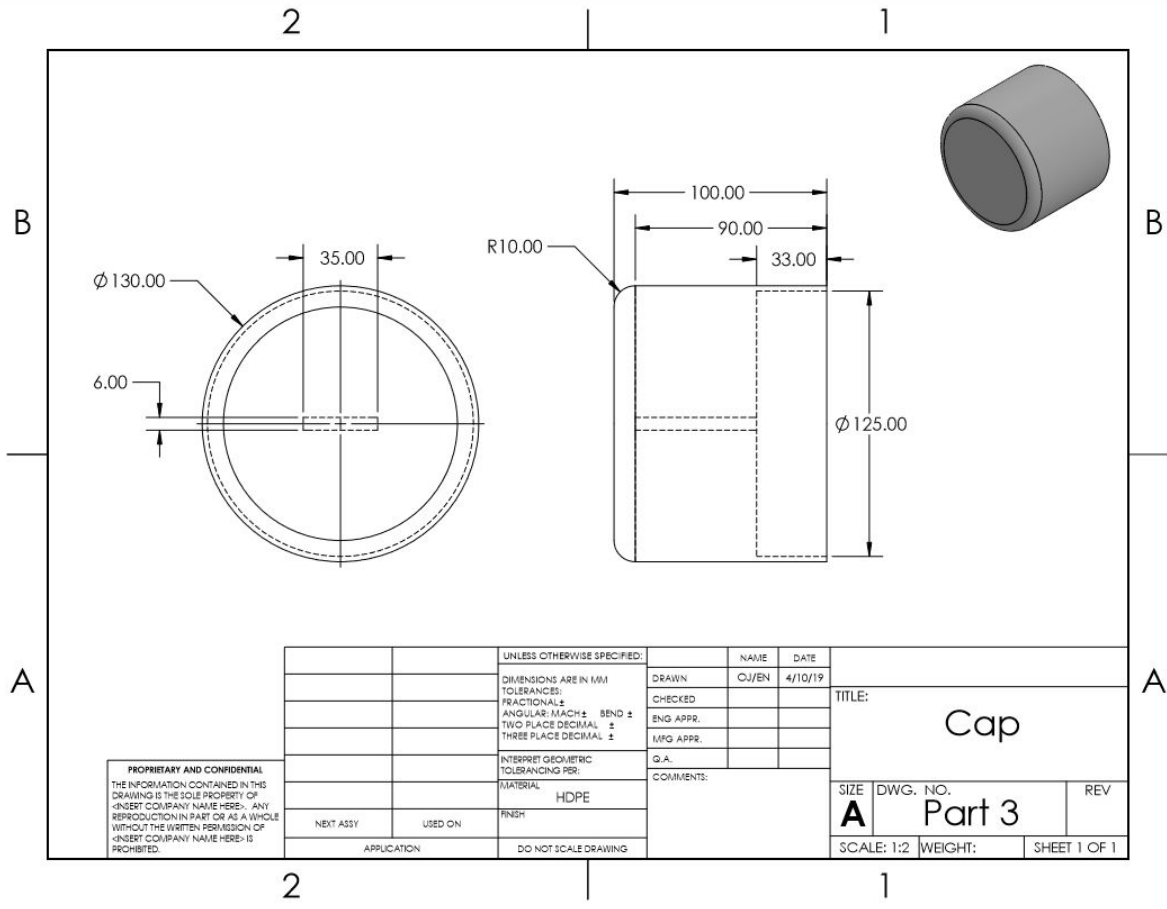


Figure 40: Drawing of Cap

The first cap is designed to cover one end of the housing and insert the pin into. It remains stationary with the housing.

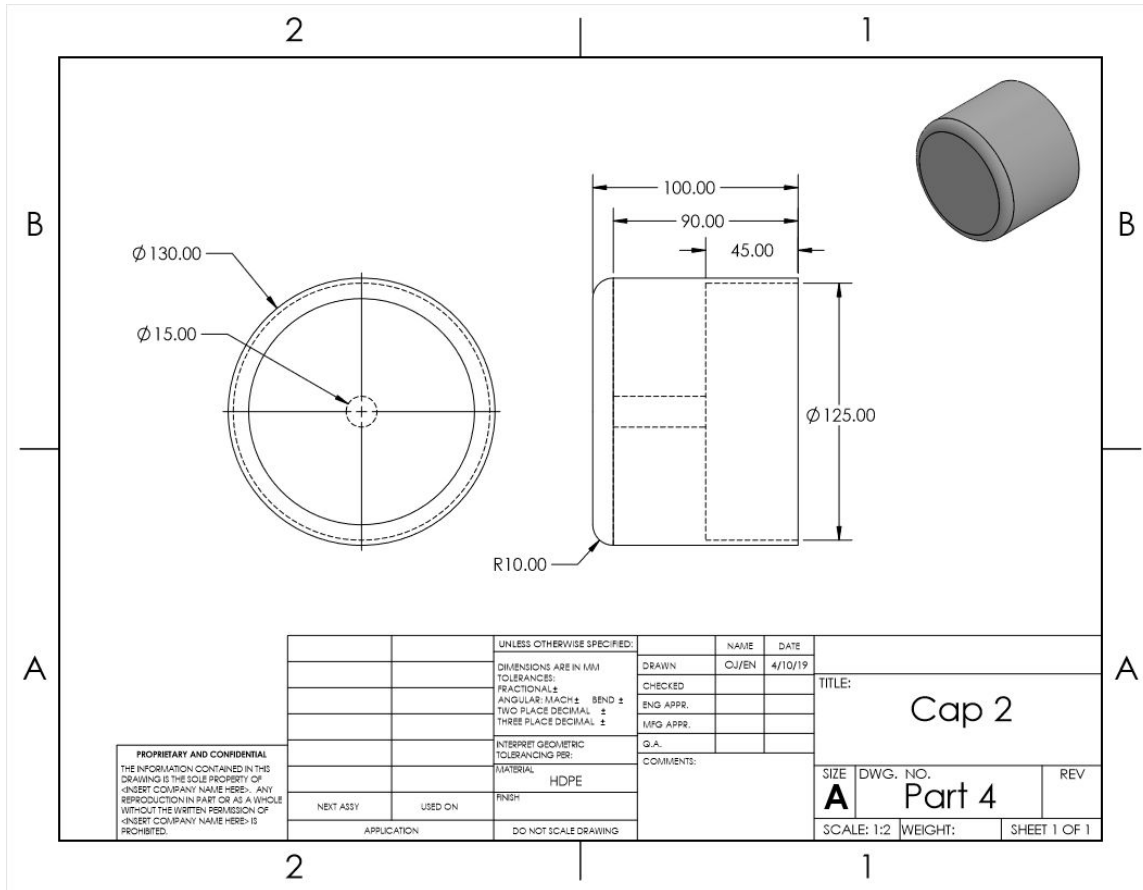


Figure 41: Drawing of Cap 2

The second cap covers the opposite end of the housing and the axle is inserted. It also remains stationary.

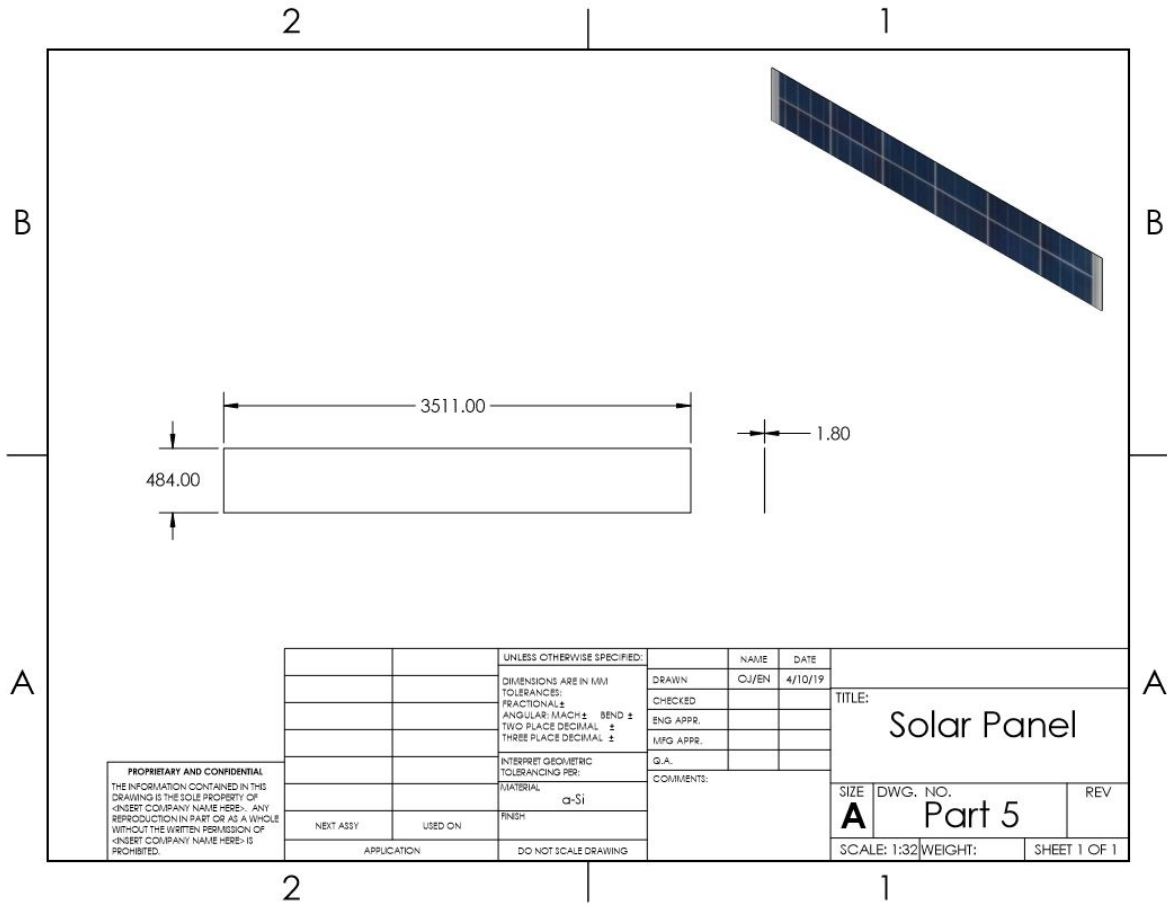


Figure 42: Drawing of Solar Panel

The solar panel was modeled based on dimensions provided by F-WAVE. They are adhered directly to the fly. This assembly depicts the fly with four panels, but can be adapted based on consumer needs. A schematic of the circuit design with four panels in parallel is shown below.

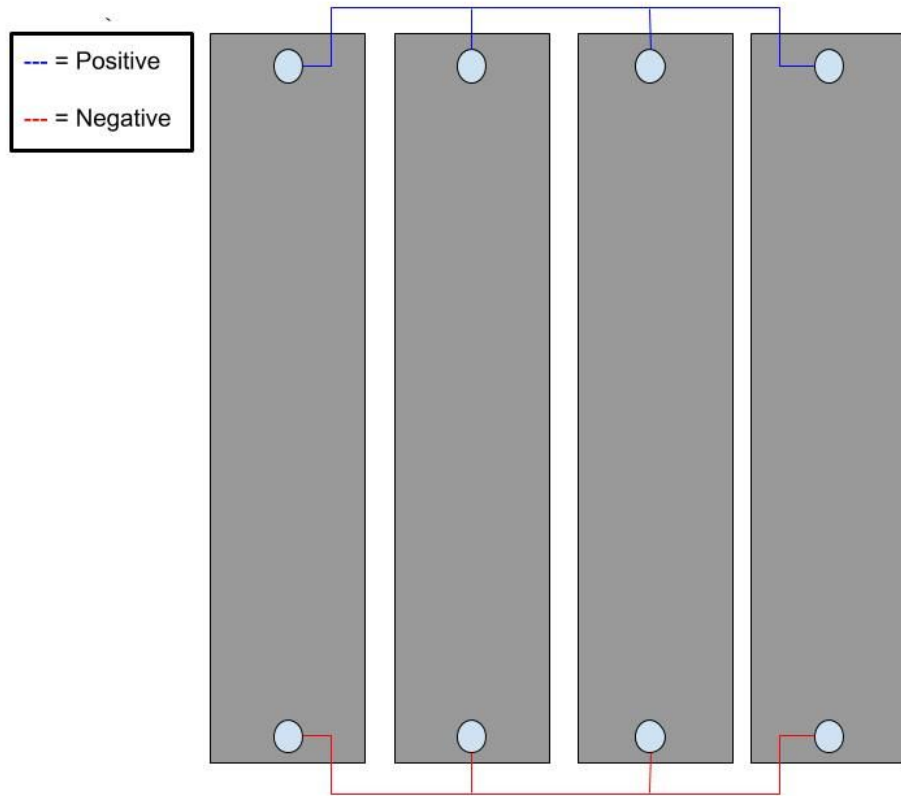


Figure 43: Schematic of the circuit design with four panels

3.3.5 Scaled Model



Figure 44: Scaled SolFly Model

A 1/10 size scaled model was created for the purposes of design realization and testing. This included a SolFly model and “Family Tent for Hot Climate” model. Components for the scaled SolFly were both obtained from existing technology and custom made. Purchase and manufacture of existing technology is outlined in the following section. Dimensions of these components were dependent on market availability, and custom parts were designed to create a

full assembly. Custom parts were modelled in SolidWorks and produced with additive manufacturing. Prior to 3D-printing the components, designs were iterated in order to minimize material usage and production time. Figure 45 compares the initial and final designs of a successfully optimized part. A model solar circuit was also designed with the intent to charge a cell phone, and later tested to confirm circuit performance.

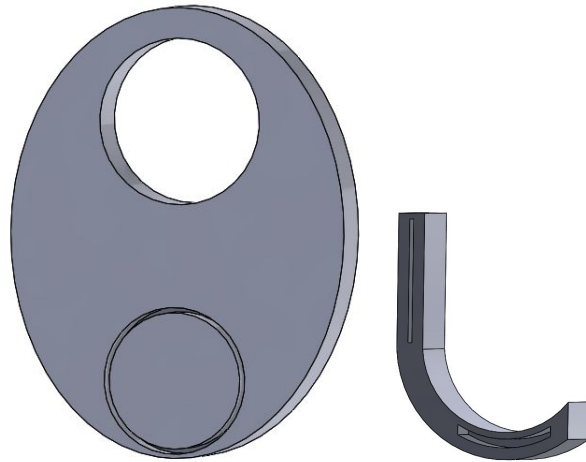


Figure 45: Optimization of Connector Design for 3D Printing

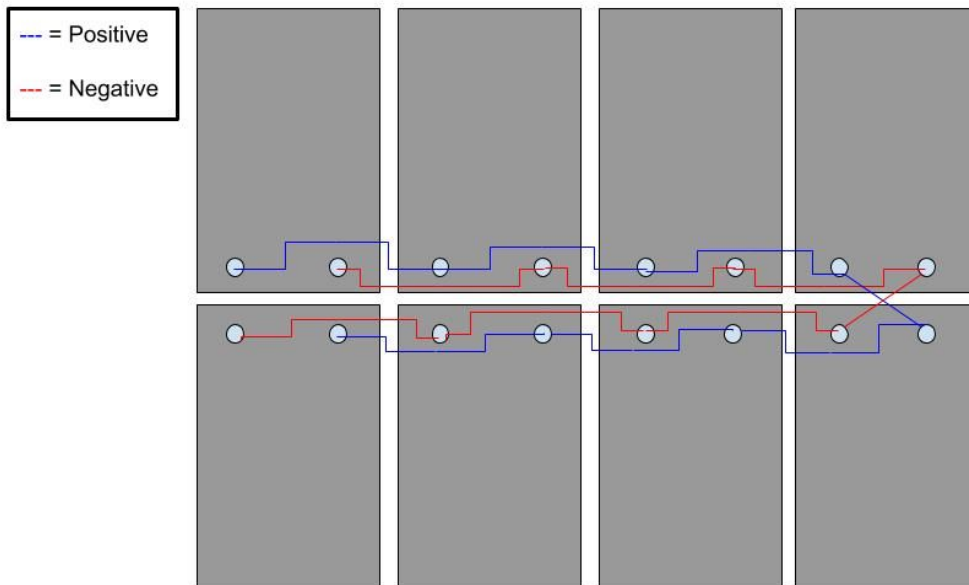


Figure 46: Schematic of Model Solar Circuit

3.4 Manufacture & Shipment

SolFly was designed using a combination of existing technology and custom components. The manufacturing processes for each part would differ slightly for the full scale prototype compared to the model. Processes for each are outlined below.

3.4.1 Solar Panels

The full scale prototype uses thin film solar panels produced by F-WAVE, a company that purchased the solar branch of Fuji Electric. The factory, based in Kumamoto, Japan, uses a roll-to-roll manufacturing method to produce the solar cells on an ethylene tetrafluoroethylene (ETFE) substrate[1]. ETFE is a corrosion resistant polymer used to protect the solar cells. Roll to roll is a cost-effective processing method commonly used in production of thin film amorphous silicon photovoltaics. By this method, electronic devices are created on a flexible steel or plastic foil. Plastic foils are advantageous for solar cell manufacture because holes can be punched through the flexible substrate for electrical connections [37].



Figure 47: F-WAVE Solar Cell Manufacturing Facility in Kumamoto, Japan [7]

The panels used for the small scale model circuit are produced by the company Jiang and sold through Amazon. These panels are made of monocrystalline silicon and also laminated with an ethylene tetrafluoroethylene (ETFE) polymer layer [1]. Processing information is not provided by the manufacturer, but it can be assumed that a similar production method is used.

3.4.2 Tent Fly

Manufacture of a tent fly is a multi-stage process. Because nylon is a man-made polymer, the process begins in chemical plants. Large organic molecules, adipic acid and hexamethylenediamine, are reacted in a pressure vessel known as an autoclave at about 285°C. When combined, these molecules undergo the process of condensation polymerization where they form a larger molecule, nylon 6,6. The nylon sheet or ribbon formed by this process is then shredded into chips. The chips are melted and spun through a spinneret to make them into fibers

to be woven together [38]. Ripstop fabrics are woven in a crosshatch pattern to reduce tearing. Ripstop nylon specifically is interwoven with strong yarns that serve as reinforcements to prevent spread of tears [29].

The prototype tent fly can be purchased in bulk from a company such as Ripstop by the Roll. Wholesale prices are cost effective when producing a product at large scale. For the scaled model, a comparable ripstop nylon tent fly is purchased from Amazon and cut to size.

3.4.3 Spring Mechanism

The spring, rod, pin, and axle are metal parts. Custom springs can be purchased from James Spring & Wire Co. The manufacturer explains that stainless steel is often used to make springs due to its durability, rust resistance, and high yield strength. Steel springs are made by drawing a heated metal bar through dies until the desired diameter is obtained. The wire is tempered and hardened according to design needs [14]. The spring properties required for this application are discussed in section 4.2. The rod, pin, and axle are made of extruded aluminum. All metal components of the spring mechanism were obtained from a spring roller shade for the scaled model.

3.4.4 Housing and Connectors

The housing and connectors are custom-designed components made of HDPE. As previously mentioned, one of the reasons for selecting HDPE was that it is easy to fabricate. The plastic prototype parts can be injection molded. Injection molding is the most common method of manufacture for plastic parts. Through this process, raw powdered or granular plastic is heated to soften the material, then forced into a mold. The material hardens to the desired shape inside the mold and can then be removed. For the scaled model, these parts were made by additive manufacturing using polylactic acid (PLA)[2].

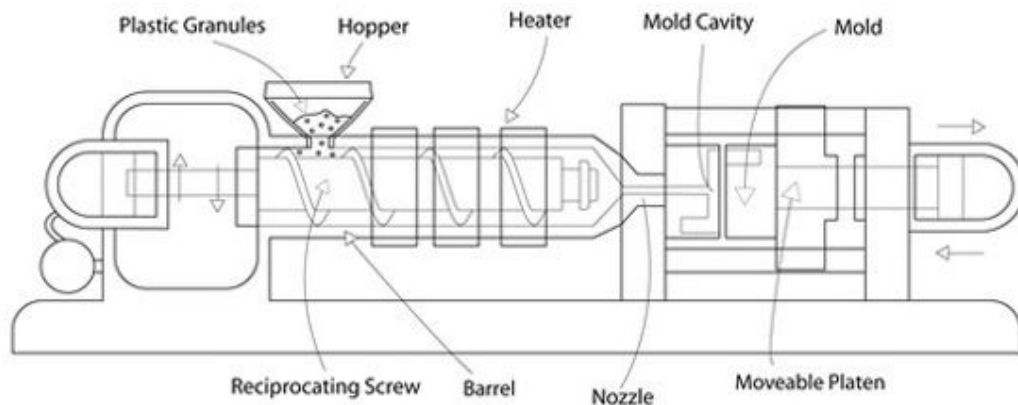


Figure 48: Injection Molding Machine [22]

3.4.5 Transportation

Transportation of the device must be taken into consideration after the product is manufactured. The dimensions of UNHCR certified cargo trucks that would transport these devices are: 8.920m x 2.470m x 2.600m (LxWxH). Dimensions of the SolFly container are: 4m x .125m x .125m (LxWxH). Based on dimensions, there is enough space for up to 790 SolFly products. However, the cargo truck also has a weight limit of 9.5 metric tons. Using the weight of the SolFly product, 32 kilograms, it is determined the cargo truck can hold at most 290 SolFly products. To avoid approaching the weight capacity, each cargo shipment can transport roughly 250 SolFly products [31].

4.0 Analysis

To provide an empirical explanation and confirm the integrity of the SolFly product, analyses were conducted for four factors: structural, mechanical, electrical and cost. The first calculations are a static structural analysis. Beam deflection is assessed to determine a weight limit for the SolFly system. Deflection simulation is performed using ANSYS software along with stress formulas. Next, wind forces are taken into consideration. Calculations are conducted to determine the wind force required to tip the tent and compared to wind forces in target locations. Effects of drag on the proposed geometry are also assessed. Next the spring mechanism is assessed to ensure proper functionality. Energy output of the photovoltaic system is gauged to show the system's scale of application. In this case, the electrical analysis shows the energy output, in joules, of the full-size SolFly as well as the model. The energy output is then compared to energy requirements for a number of potential applications. The SolFly product must provide substantial energy, and be financially feasible for implementation. Cost is analyzed to show how the SolFly system compares to current products.

4.1 Structural

The center beam of the tent plays an important role in the tent structure. Along with the adjoining poles, the center beam bears the weight of the tent fabric. Side poles and guy lines are used to maintain shape, but do not bear the weight of the structure. Static structural calculations and simulations were performed to ensure the center beam is not compromised under additional weight subjected by the SolFly device. The tipping force of the tent was also determined to ensure the tent structure can withstand even the most extreme weather of the target locations.

4.1.1 Beam Deflection

The maximum deflection of the tent center beam caused by the weight of the SolFly device was calculated by method of superposition. Then, the point of plastic deformation was calculated. There is no allowable deflection for this design, however, so tent reinforcements were simulated and compared to the current design.

The center beam is four meters long, and is connected to three center poles at distances of 0 m, 2 m and 4 m from either end. Figure 49 below depicts the distributed weight acting on the beam. To simplify the system, calculations were performed using half of the beam with fixed supports at either end, rather than the total 4 m with an additional pole in the middle.

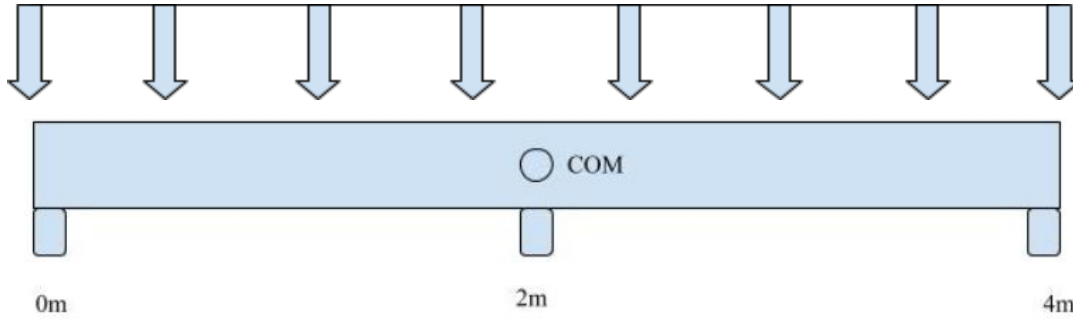


Figure 49: Schematic of Center Beam with Three Fixed Supports, COM, and Distributed Weight

A distributed load due to the weight of SolFly is calculated over the 2 m section. The load of the SolFly addition is determined by adding weights of the solar panel, fly material and spring mechanism. Tent area is approximated using tent dimensions of 6.6m x 4m. Half of this mass is then applied as a distributed load to the center beam, to account for the partition.

Calculations for the full size SolFly:

Weight Calculations:

Equation:

$$W_{\text{solfly}} = W_{\text{panel}} + W_{\text{fly}} + W_{\text{spring mechanism}}$$

Variables:

$$W_{\text{SolFly without solar panels}} = 19.40 \text{ kg}$$

$$W_{\text{solar panels}} = 12.8 \text{ kg}$$

Solved:

$$W_{\text{solfly}} = W_{\text{psolar anel}} + W_{\text{SolFly without panels}} = 19.40 + 12.8 = \mathbf{32.2 \text{ Kg}}$$

This weight was then used to determine the max deflection and max stress as follows.

Deflection SolFly:

Equation:

$$\text{Deflection} = \delta = (5/384) * (W * l^3/EI)$$

Variables:

Weight	$W = 32.2kg * 9.8m/s^2$
Elastic Modulus	$E = 200 \text{ GPa} = 200 * 10^9 \text{ N/m}^2$
Length of beam	$l = 4m/2 = 2m$
Moment of Inertia	$I = \pi * (D^4 - d^4)/64 = 9.6 * 10^{-9} m^4$
Outer diameter	$D = 0.030m$
Inner Diameter	$d = 0.028m$

Solved:

$$\begin{aligned} \delta &= (5/384) * [(32.2 \text{ kg} * 9.8 \text{ m/s}^2) * (2m)^3 / (200 * 10^9 \text{ N/m}^2) * (9.6 * 10^{-9} \text{ m}^4)] = \\ &= (5/384) * [(315.56N * 8m^3)/1920Nm^2] = .0171 \text{ m} = \mathbf{17.1 \text{ mm}} \end{aligned}$$

Max Stress

Equation:

$$\text{Max Stress} = W * l/8 * Z$$

Variables:

Weight	$W = 32.2kg * 9.8m/s^2$
Length of beam	$l = 4m/2 = 2m$
Edge distance	$z = 0.015m$

Section modulus of cross section $Z = I/z = 9.6 * 10^{-9} m^4 / .015 m = 6.393 * 10^{-7} m^3$

Solved:

$$\begin{aligned} &= W * l/8 * Z = (32.2kg * 9.8m/s^2 * 2m)/(8 * 6.393 * 10^{-7} m^3) \\ &= 631.12Nm/5.1144 * 10^{-6} m^3 = 123.4 * 10^6 N/m^2 = \mathbf{123.4 \text{ MPa}} \end{aligned}$$

Deflection to Plastic Deformation:

Equation was found for a beam supported at either end with a midpoint load

Equation:

$$\text{max. deflection} = (W * l^3)/(48 * E * I)$$

Variables:

Weight	$W = 32.2 \text{ kg} * 9.8m/s^2$
Elastic Modulus	$E = 200 \text{ GPa} = 200 * 10^9 \text{ Pa}$
Length	$l = 4m/2 = 2 \text{ m}$
Moment of Inertia	$I = \pi * (D^4 - d^4)/64 = 9.6 * 10^{-9} m^4$
Outer diameter	$D = 0.030m$

Inner Diameter $d = 0.028m$

Solved:

$$\begin{aligned} &= (W * l^3)/(48 * E * I) \\ &= (32.2 \text{ kg} * 9.8m/s^2) * (2^3 m^3)/(48 * (200 * 10^9 Pa) * (9.6 * 10^{-9} m^4)) \\ &= 0.0274m = \mathbf{27.4 \text{ mm}} \end{aligned}$$

Weight to cause Plastic Deformation:

Equation:

$$deflection = 5 * w * l^3 / 384 * E * I$$

$$\text{Solved for } W = deflection * 384 * E * I / 5 * l^3$$

Variables:

Deflection $\delta = 0.0214m$

Weight $W = 32.2 \text{ kg} * 9.8m/s^2$

Elastic Modulus $E = 200 \text{ GPa} = 200 * 10^9 \text{ Pa}$

Length $l = 4m/2 = 2 \text{ m}$

Moment of Inertia $I = \pi * (D^4 - d^4)/64 = 9.6 * 10^{-9} m^4$

Outer diameter $D = 0.030m$

Inner Diameter $d = 0.028m$

Solved:

$$\begin{aligned} W &= deflection * 384 * E * I / 5 * l^3 \\ &= [0.0274m * 384 * (200 * 10^9 Pa) * (9.6 * 10^{-9} m^4)] / (5 * 2^3 m^3) \\ &= 504.9 \text{ N} \end{aligned}$$

Solved for Mass $m = W/g = 504.9N / 9.8m/s^2 = \mathbf{51.51kg}$

All the same calculations were performed for the scaled model as follows:

Deflection:

Equation:

$$\text{Deflection} = \delta = (5/384) * (W * l^3/EI)$$

Variables:

Weight $W = .02778kg * 9.8m/s^2$

Elastic Modulus $E = 200 \text{ GPa} = 200 * 10^9 \text{ N/m}^2$

Length of beam $l = .4m/2 = .2m$

Moment of Inertia $I = \pi * (D^4 - d^4)/64 = 4.528 * 10^{-12} m^4$

Outer diameter $D = 0.003175m$

Inner Diameter $d = 0.00175m$

Solved:

$$\delta = (5/384) * [(0.02778 \text{ kg} * 9.8 \text{ m/s}^2) * (.2m)^3 / (200 * 10^9 \text{ N/m}^2) * (4.528 * 10^{-12} \text{ m}^4)]$$

$$= (5/384) * [(0.2722N * .008m^3)/.9056m^2] = 3.13 * 10^{-5}m. = \mathbf{0.0313mm}$$

Max Stress

Equation:

$$\text{Max Stress} = W * l/8 * Z$$

Variables:

Weight $W = .02778kg * 9.8m/s^2$

Length of beam $l = .4m/2 = .2m$

Edge distance $z = 0.0015875m$

Section modulus of cross section $Z = I/z = 4.528 * 10^{-12} \text{ m}^4 / .0015875m = 2.85 * 10^{-9}m^3$

Solved:

$$= W * l/8 * Z = (.02778kg * 9.8m/s^2 * .2m)/(8 * 2.85 * 10^{-9}m^3)$$

$$= .0545Nm/2.28 * 10^{-8}m^3 = .239 * 10^6N/m^2 = \mathbf{0.239 MPa}$$

Deflection to Plastic Deformation:

Equation was found for a beam supported at either end with a midpoint load

Equation:

$$\text{max. deflection} = (W * l^3)/(48 * E * I)$$

Variables:

Weight $W = .02778 \text{ kg} * 9.8m/s^2$

Elastic Modulus $E = 200 \text{ GPa} = 200 * 10^9 \text{ Pa}$

Length $l = .4m/2 = .2 \text{ m}$

Moment of Inertia $I = \pi * (D^4 - d^4)/64 = 4.528 * 10^{-12}m^4$

Outer diameter $D = 0.003175m$

Inner Diameter $d = 0.00175m$

Solved:

$$= (W * l^3)/(48 * E * I)$$

$$= (.02778 \text{ kg} * 9.8m/s^2) * (.2^3m^3)/(48 * (200 * 10^9Pa) * (4.528 * 10^{-12}m^4))$$

$$= 5.01 * 10^{-5}m = \mathbf{.0501mm}$$

Weight to cause Plastic Deformation:

Equation:

$$\text{deflection} = 5 * w * l^3/384 * E * I$$

$$\text{Solved for } W = \text{deflection} * 384 * E * I / 5 * l^3$$

Variables:

Deflection	$\delta = 0.0000501m$
Weight	$W = X \text{ kg} * 9.8m/s^2$
Elastic Modulus	$E = 200 \text{ GPa} = 200 * 10^9 \text{ Pa}$
Length	$l = .4m/2 = .2 \text{ m}$
Moment of Inertia	$I = \pi * (D^4 - d^4)/64 = 4.528 * 10^{-12}m^4$
Outer diameter	$D = 0.003175m$
Inner Diameter	$d = 0.00175m$

Solved:

$$\begin{aligned} W &= \text{deflection} * 384 * E * I / 5 * l^3 \\ &= [0.0000501m * 384 * (200 * 10^9 \text{ GPa}) * (4.528 * 10^{-12}m^4)] / (5 * .2^3m^3) \\ &= .431N \end{aligned}$$

$$\text{Solved for Mass } m = W/g = .431N / 9.8m/s^2 = \mathbf{.0440kg}$$

Ansys simulation was performed to determine a diameter at which there would be no deflection, this was achieved by reinforcing the beam. Because the beam is already made of structural steel, rather than change its material, the beam was thickened.

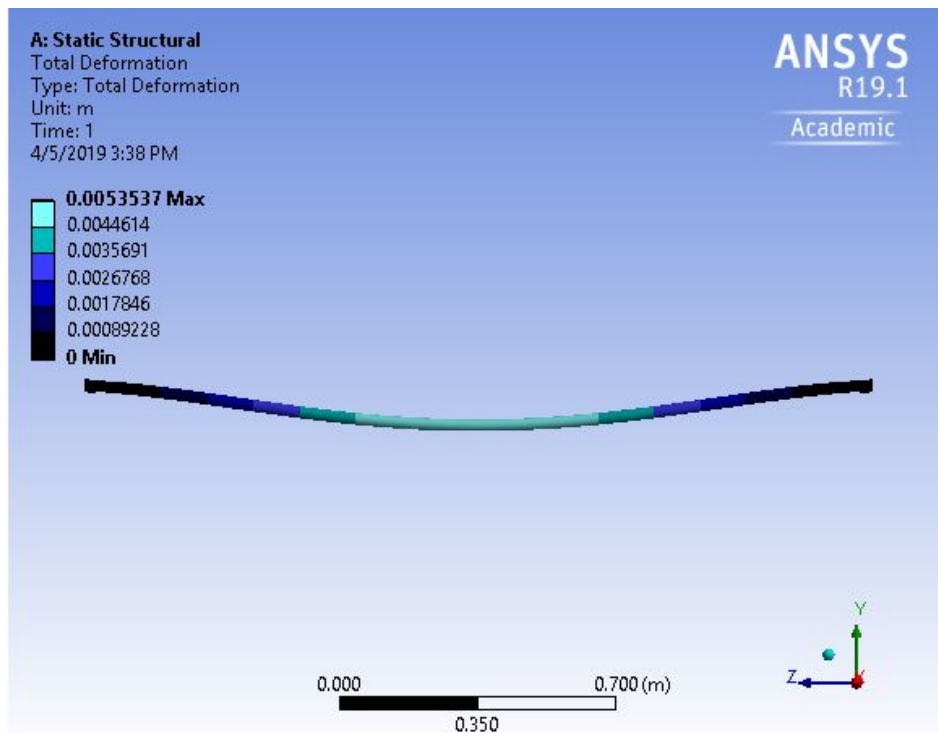


Figure 50: Original ANSYS Results for Tent Beam Deflection with SolFly

largest deflection = 0.0053537 m ~5.35 mm

Outer Diameter = 30 mm

Inner Diameter = 28 mm

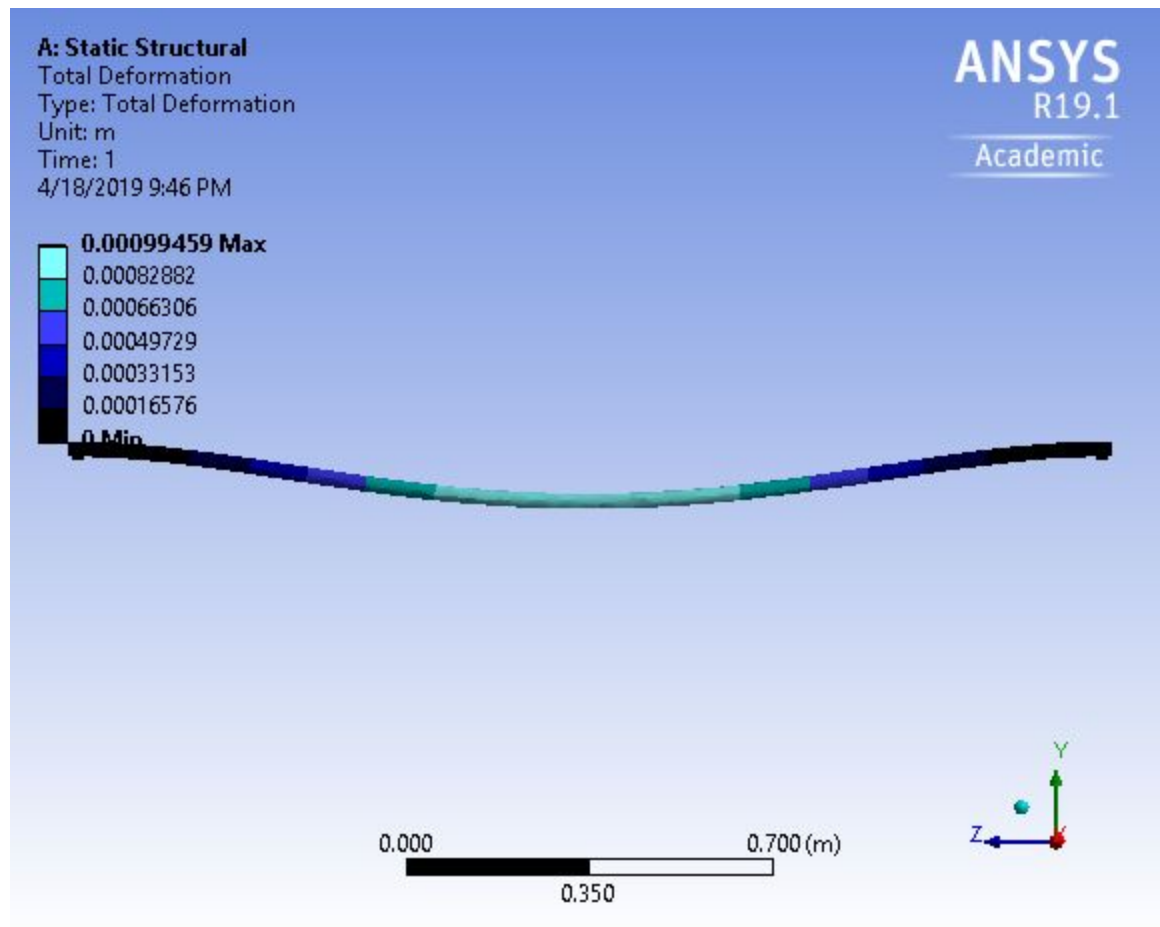


Figure 51: Reinforced ANSYS Results for Tent Beam Deflection with SolFly

Largest Deflection = 0.0009945m ~ .9945 mm

Outer Diameter = 30 mm

Inner Diameter = 20 mm

Altering the inner diameter from 28mm to 20mm changed maximum deflection from 5.35mm to 0.9945 mm. This new deflection is miniscule enough to not threaten structural integrity of the beam. ANSYS simulation is considered more accurate than simple beam calculation because it assesses specific geometry rather than only cross-sectional area.

To determine a safety factor for the design, maximum stress experienced by the reinforced beam is calculated. The ultimate stress of steel is then divided by this value.

Max Stress for Reinforced Beam

Equation:

$$\text{Max Stress} = W * l/8 * Z$$

Variables:

Weight	$W = 32.2\text{kg} * 9.8\text{m/s}^2$
Length of beam	$l = 4\text{m}/2 = 2\text{m}$
Edge distance	$z = 0.015\text{m}$
Moment of Inertia	$I = \pi * (D^4 - d^4)/64 = 3.19 * 10^{-8}\text{m}^4$
Outer diameter	$D = 0.030\text{m}$
Inner Diameter	$d = 0.020\text{m}$

Section modulus of cross section $Z = I/z = 3.19 * 10^{-8}\text{m}^4 / .015\text{m} = 2.13 * 10^{-6}\text{m}^3$

Solved:

$$\begin{aligned} W * l/8 * Z &= (32.2\text{kg} * 9.8\text{m/s}^2 * 2\text{m}) / (8 * 2.13 * 10^{-6}\text{m}^3) \\ &= 631.12\text{Nm} / 1.704 * 10^{-5}\text{m}^3 = 37036385\text{N/m}^2 = \mathbf{37.04\text{MPa}} \end{aligned}$$

Safety Factor

Equation:

$$n = \text{Strength} / \text{Max Stress}$$

Variables:

Strength	= 400 MPa
Max Stress	= 37.04 MPa

Solved:

$$n = \text{Strength} / \text{Max Stress} = 420\text{MPa} / 37.04\text{MPa} = \mathbf{11.34}$$

This design is proven to be safe with a safety factor of 11.34.

4.1.2 Tipping Force

Calculations regarding the wind are conducted to determine the force required to tip the UNHCR tent both with and without the SolFly addition. Additionally, the tipping force is compared to the wind force experienced in the potential target locations, Mafraq, Jordan and Windhoek, Namibia. The variables are assumed to be the most extreme weather conditions experienced within the Mafraq region of Jordan, which is comparable with extreme wind speeds in Namibia. The wind speed is found to be 7.6 m/s, which is only surpassed a handful of days annually [11]. The tipping force is compared to the wind force experienced to assess the effect of the SolFly addition on the UNHCR tent.

Wind force was found using the following calculations:

$$\text{Force of the Wind} \quad F_w = P * A \text{ [N]}$$

Height	$h = 2.2m$
Width	$w = 4m$
Area	$h * w = 8.8m^2$
Density of air	$\rho = 1.2 kg/m^3$
Wind speed	$v = 7.6m/s$
Dynamic Pressure	$P = (1/2) * \rho * v^2 = .5 * (1.2 kg/m^3) * (7.6m^2/s^2) =$ $P = 34.65 kg/ms^2$
Force of the Wind (solved)	$F_w = P * A = 34.65kg/ms^2 * 8.8 m^2 = 304 N$

The forced required to tip is calculated using the center of masses both horizontally and vertically, and uses the mass of all the tent components to determine the force to tip.

Tent Without SolFly:

Force to tip	$F = w * w_{COM}/h_{COM} [N]$
Height(Center of Mass)	$h_{COM} = 1.58 m$
Width(center of mass)	$w_{COM} = 2 m$
Mass	$m = 32.72 kg$
Weight	$w = 32.72 kg * 9.8 m/s^2 = 320.69 N$
Force to tip (solved)	$F = (320.69 * 2)/(1, 58) = 405.94 N$

Tent with SolFly:

Force to tip	$F = w * w_{COM}/h_{COM} [N]$
Height(Center of Mass)	$h_{COM} = 1.58 m$
Width(center of mass)	$w_{COM} = 2m$
Mass	$m = m(tent) + m(solfly) =$ $32.72kg + (32.2kg) = 64.92 kg$
Weight	$w = 64.92 kg * 9.8 m/s^2 = 636.216 N$
Force to tip (solved)	$F = (636.216 * 2)/(1, 58) = 805.33 N$

The force required to tip the UNHCR tent in both scenarios exceeds the 304 N wind force that represents a worst case scenario in the Mafraq region of Jordan. The force to tip for the tent with the SolFly addition increases due to the additional mass of the SolFly.

Additionally, the combined force of drag force due to wind with the horizontal wind force must also remain under threshold force to tip to maintain structural integrity.

4.2 Spring Mechanism

The appropriate tension force for the spring is determined using Hooke's Law. This law states that the torque is equal to the spring constant multiplied by the angle of twist from its equilibrium position in radians. Applied torque can be calculated by multiplying the lever arm by force applied. Calculations were performed for both the scaled model and SolFly prototype.

Torque Equation:

$$T = rF \sin(\Theta)$$

Where

$$T = \text{Torque applied} = ?$$

$$r = \text{Radius of spring mechanism} = 20 \text{ mm}$$

$$F = \text{Force applied} = 246.5 \text{ N}$$

$$c = \text{Circumference of pipe} = \pi d = \pi * 120 \text{ mm} = 376.8 \text{ mm}$$

$$l = \text{Length of fly} = 7 \text{ m}$$

$$\begin{aligned} \Theta &= \text{Degrees of displacement} = l/c = (7 \text{ m} / 376.8 \text{ mm}) * 360^\circ \\ &= 18.58 * 360^\circ = 6,687.90 = 116.725 \text{ rad} \end{aligned}$$

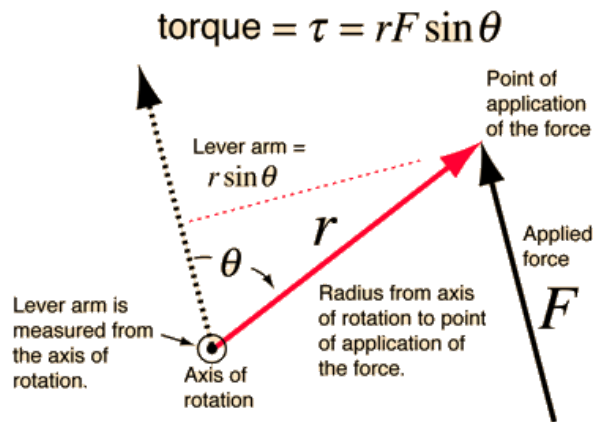


Figure 52: Diagram of Torque Calculation [30]

Solved:

$$T = rF \sin(\Theta)$$

$$T = (.04 \text{ m}) * (246.5 \text{ N}) * \sin(116.725)$$

$$T = (9.86 \text{ Nm}) * (-0.467)$$

$$T = -4.606 \text{ Nm} = -4,606 \text{ Nmm}$$

Hooke's Law:

$$T = -k\phi$$

Where

$$T = \text{Torque applied} = -4.606Nm$$

$$k = \text{Torsional spring constant} = ?$$

$$\phi = \text{Radians of displacement} = l/c = (7m/376.8mm) * 360^\circ \\ = 18.577 * 360^\circ = 6687.90 = 116.725 \text{ radians}$$

$$k = -T/\phi$$

$$k = (4.606 / 116.725)$$

$$k = \mathbf{0.0395 \text{ Nm/rad}}$$

Calculations for Scaled Model:

Torque Equation:

$$T = rF \sin(\Theta)$$

Where

$$T = \text{Torque applied} = ?$$

$$r = \text{Radius of spring mechanism} = 20 \text{ mm}$$

$$F = \text{Force applied} = 0.272 \text{ N}$$

$$c = \text{Circumference of pipe} = \pi d = \pi * 40mm = 125.6mm$$

$$l = \text{Length of fly} = 700 \text{ mm}$$

$$\Theta = \text{Degrees of displacement} = l/c = (700mm/125.6mm) * 360^\circ \\ = 5.573 * 360^\circ = 2,006.37$$

Solved:

$$T = rF \sin(\Theta)$$

$$T = (.020m) * (0.272N) * (\sin(2006.37))$$

$$T = (.0 - 544Nm) * (-0.44416612467)$$

$$T = -0.00241626 \text{ Nm} = -2.41626 \text{ Nmm}$$

Hooke's Law:

$$T = -k\phi$$

Where

$$T = \text{Torque applied} = -0.00241626 \text{ Nm}$$

$$k = \text{Torsional spring constant} = ?$$

$$\phi = \text{Radians of displacement} = l/c = (700mm/125.6mm) * 360^\circ \\ = 5.573 * 360^\circ = 2,006.37 = 35.01 \text{ radians}$$

$$k = -T/\phi$$

$$k = (0.00241626 / 35.01)$$

$$k = \mathbf{0.00006902 \text{ Nm/rad}}$$

The prior calculations establish a minimum spring constant requirement in order to overcome the weight of the tent fly for both the model and prototype. The minimum spring constant for the prototype is $k = \mathbf{0.0395 \text{ Nm/rad}}$. The minimum spring constant for the scaled model is $k = \mathbf{0.00006902 \text{ Nm/rad}}$. The k value of the spring must be found by testing.

4.3 Electrical

The most valuable aspect of the SolFly system is its solar components, providing electricity for a single family or multiple families to suit their needs. Additionally, SolFly does not take up any further ground space, and attaches directly to the tent frame as a space efficient product. Calculations are conducted assuming with a panel of dimensions 3.399m x .460m. This solar panel corresponds to option 5 in tables 2,3 and 4.

Electrical Calcs:

Wattage Rating	$1 \text{ panel} = 70 \text{ watts}$
Area of solar panel	$3.399 \text{ m} * 0.460 \text{ m} = 1.56 \text{ m}^2$
Watts rate per area	$44.87 \text{ w/m}^2 \text{ [watts/area]}$
Height	7.0 m
Width	4.0 m
Area available	$(h * w) = 7.0 \text{ m} * 4.0 \text{ m} = 28.0 \text{ m}^2$
Area used	$4 \text{ panels} * 1.56 \text{ m}^2 = 6.24 \text{ m}^2$

The tent fly can comfortably fit 15 solar cells, but due to weight concerns 4 are implemented

$$\text{Wattage} \quad \# \text{ of solar cells} * (\text{Area} * W/\text{Area}) = 4 * (44.87 * 1.56) = 280 \text{ w}$$

Amount of energy produced on an average day:

Hours of usable sunlight were found using the insolation map found in Figure 53.

Energy produced	$E = w * t * 3600\text{s/hr} \text{ [J]}$
Hours of sunlight	$t = (5 + 5.9)/2 = 5.45 \text{ hr}$
Wattage	280 watts
Energy produced	$E = 280\text{w} * 5.45\text{hr} * 3600\text{s/hr} = 5,493,600 \text{ J}$

World Insolation Map

This map shows the amount of solar energy in hours, received each day on an optimally tilted surface during the worst month of the year. (Based on accumulated worldwide solar insolation data.)

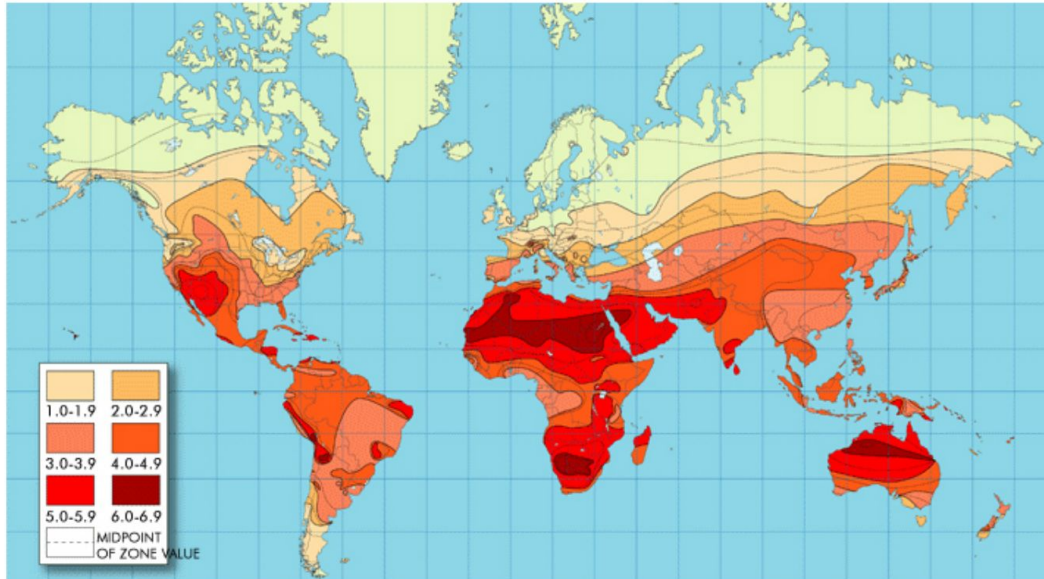


Figure 53: World Insolation Map Showing Average Hours of Sunlight Per Day [36]

Power requirements for various devices were established in the design criteria section. These devices included a small clothes washer, charging a cell phone, boiling water, and powering an LED bulb. Using those energy requirements along with the energy calculations above, it is deduced that one SolFly unit can power a washer for 4 cycles, charge 150 iPhones, boil 16.6 liters of water, or run a 60 watt light bulb for 25.4 hours.

The SolFly is able to provide electricity for a number of household applications with four solar panels. Below, in Table 6, the wattage, area, weight and number of lightbulbs which can be powered per number of solar panels are expressed. Although there is enough area on the tent fly for 16 solar panels, there are weight restrictions due to the current tent frame. 51 kg will cause plastic deformation, but beam deflection should be avoided entirely. The device should also not be too heavy to transport.

In addition, there is the possibility of a SolFly attachment extended over both sides of the tent. In this case, the weight of two SolFly devices must be considered. As a result, it was determined that four solar panels will provide ample energy (280W) to perform a number of tasks and also leave the additional weight well below the 50 kilogram threshold. When reinforced, the center beam would experience no deflection under the weight and a single SolFly unit would be easy for two people to lift.

Table 6. Specifications per Number of Solar Panels

Panels	Weight (Kg)	Watts (W)	Area (m ²)	Light bulbs (10W)
1	3.2	70	1.56	7
2	6.4	140	3.12	14
3	9.6	210	4.68	21
4	12.8	280	6.24	28
5	16	350	7.8	35
6	19.2	420	9.36	42
7	22.4	490	10.92	49
8	25.6	560	12.48	56
9	28.8	630	14.04	63
10	32	700	15.6	70
11	35.2	770	17.16	77
12	38.4	840	18.72	84
13	41.6	910	20.28	91
14	44.8	980	21.84	98
15	48	1050	23.4	105
16	51.2	1120	24.96	112

4.4 Drag Force Calculations

The UNHCR “Family Hot Climate Tent” has been tested to ensure its structural integrity, but with the addition of the SolFly it is important to again confirm the tent is safe for use. With this in mind, it was important to generate a range of drag forces. Drag force depends on the velocity, drag coefficient, fluid density and reference area of an item. The calculations used the drag force equation:

$$F_d = C_d * A * (\rho * v^2) / 2$$

The wind velocity is variable, and calculations were performed up to 50 m/s, far above the maximum 13 m/s experienced in the target regions [11]. The fluid density of air was assumed to be 1.225 kg/m³. The reference area of the fully extended fly was held constant at 0.28 m². The drag coefficient, determined by the test subject’s geometry, is the most challenging variable to assess. In this scenario the drag coefficient used was 0.80 and the reference geometry is a cube

lifted slightly above the ground. The fluid density of air is 1.225 kg/m^3 . Drag force with respect to relative velocity is shown below. Drag increases parabolically with wind speed.

Additionally, using the prior tipping force calculations, the team can conclude that the tent will not tip. The calculated wind force is 304 N, and, so long as the drag force does not exceed 25 m/s, the tent without SolFly will not tip. It does not exceed the 405.94 N force required to tip. The tent with the additional weight of one SolFly device will remain intact for all calculated wind speeds, and require a force of 805.33 N to tip.

Table 7. Drag Forces at Various Velocities

Relative Velocity: v (m/s)	Drag Force: Fd (N)
5	3.43
10	13.72
15	30.87
20	54.88
25	85.75
30	123.48
35	168.07
40	219.52
45	277.83
50	343

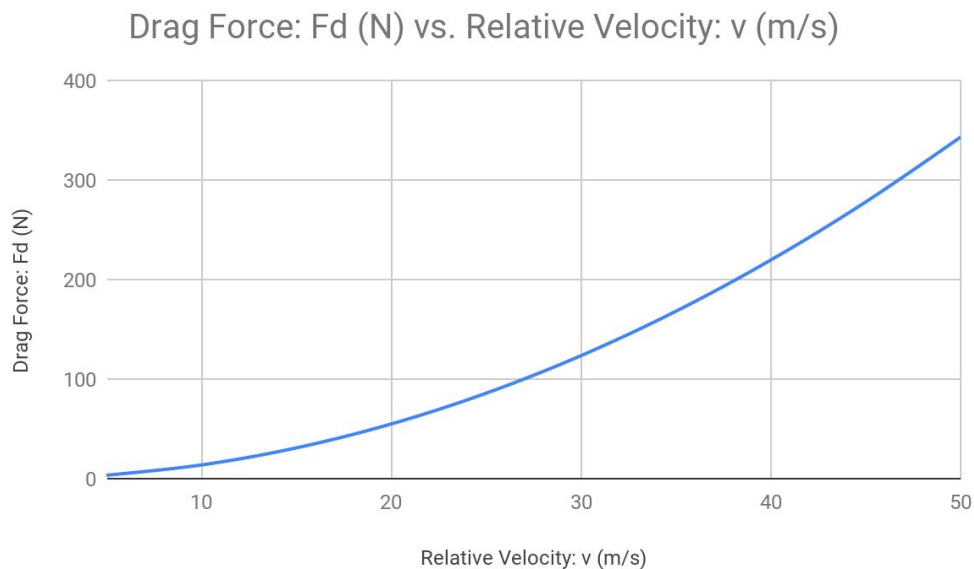


Figure 54: Graph of Drag Force vs. Velocity

4.5 Cost analysis

Investment in solar energy cannot be assessed solely by capital costs. Solar energy does not require fuel and, as a result its value is best assessed when compared to operational costs. A calculation was performed to estimate the amount of time it will take for a return on the investment of a single SolFly attachment. Many refugee camps do not have electricity, but those that do most commonly rely on diesel fuel generators or pre existing electrical infrastructure. For the purpose of this calculation, SolFly is compared to diesel fuel generators as well as electricity from a local grid in the scenario that grid access is available.

Table 8. Cost Analysis for Namibia

Namibia	Diesel	Grid	SolFly
Operation Cost (\$)	0.79 per liter	0.71 per amp	0
One Year Investment (\$)	1,231	1,943	911.2
10 Yr Total (\$)	1,402	19,430	1013.7
Time to ROI	0.740	0.469	N/A

Table 9. Cost Analysis for Jordan

Jordan	Diesel	Grid	SolFly
Operation Cost (\$)	0.86 per liter	0.66 per amp	0
One Year Investment (\$)	1,233	1,806	1041.2
10 Yr Total (\$)	1,419	18,060	1208.7
Time to ROI	0.573	0.391	N/A

The cost analyses for Namibia and Jordan are shown above. Operation cost, one year investment, and ten year total cost are compared for three energy types. The energy sources compared are: a diesel generator, grid electricity, and one SolFly. The operation cost is derived from costs local to the target region for both diesel and grid based electricity. For the SolFly, however, operation cost is derived from the efficiency of energy usage and the lifetime of its components. As components need replacing this adds into the costs of operation. Required equipment and the cost of operation for 1 year are factored into the single year investment. For diesel fuel, a diesel generator is used as the equipment. It is assumed that the equipment for grid electricity is already installed. The capital cost used for the SolFly is strictly the cost to produce the SolFly device. The ten year total includes the one year investment and operation for the following nine years. 10 years is the predicted lifespan of the torsional spring, so the analysis was conducted for that time frame. The spring could be replaced at that point, as the life

expectancy of all other component besides the battery is a minimum of 20 years. Three battery replacements are factored into the 10 year cost to avoid significant electrical losses.

Time until return on investment refers to how many years it takes for the SolFly to pay itself off when compared to other types of electricity. This was calculated by taking the one year investment of the SolFly and dividing it by the one year investment for each of the other two options. In Namibia, when compared to diesel fuel, SolFly shows return on investment in 9 months. It shows a return on investment in under six months when compared to an electric grid. In Jordan, return on investment versus diesel fuel and grid electricity are 10 months and 7 months respectively. Additionally, in each comparison the cost of using grid-based electricity is the highest, with total expenses exceeding 14 times that of a single SolFly in Jordan, and 19 times that of a Solfly unit in Namibia. This portrays how SolFly can provide alternative energy that is financially advantageous over fossil fuels.

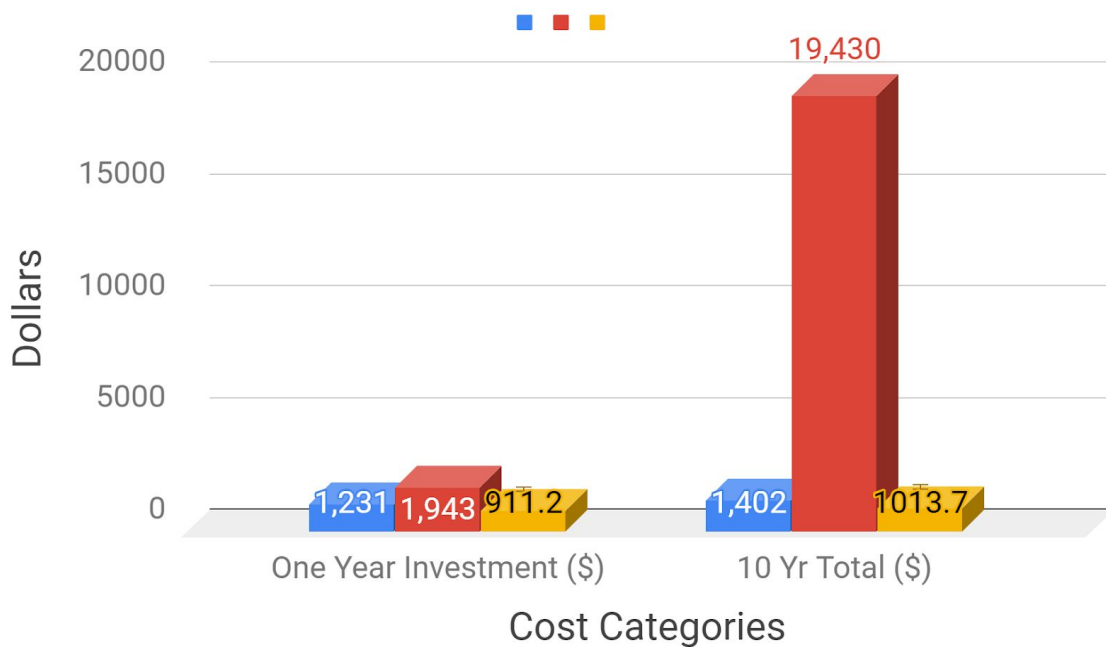


Figure 55: Cost Analysis for Refugee Camp in Namibia

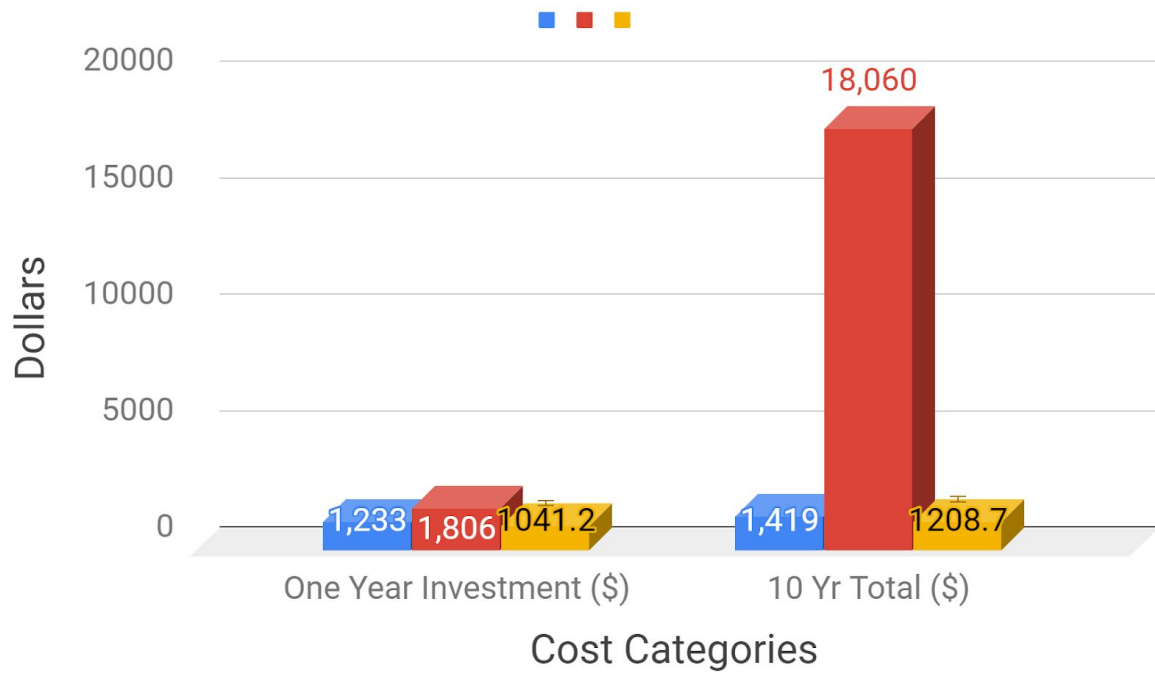


Figure 56: Cost Analysis for Refugee Camp in Jordan

5.0 Testing

5.1 Static Load Deflection

5.1.1 Purpose

To confirm the tent frame will not plastically deform under the weight of the scaled model

5.1.2 Materials

- Scaled Tent Poles and Center Beam Structure
- SolFly scaled model
- Tape Measure or Ruler

5.1.3 Procedure:

1. Measure height from ground to lowest point of center beam. Record height.
2. Attach designated weight test weight of model to center beam, so that weight is evenly distributed across beam.
3. Measure new height from ground to lowest point of center beam. Record Height.
4. Repeat procedure for three trials.

5.1.4 Data

Weight of SolFly scaled model: 27.78g

Table 10: Static Deflection Data

Trial #	Original Height (cm)	New Height (cm)	Deflection (cm)
1	21.5	21.5	0
2	21.5	21.5	0
3	21.5	21.5	0

5.1.5 Results

The measured deflection is not plastic, and the frame will not be permanently altered under the weight of the scaled model. For reference, the max allowable deflection of the scaled model is 0.0501mm

5.1.6 Conclusion

There was no deflection due to the weight of the SolFly scaled model, therefore it does not plastically deform.

5.2 Spring Constant and Tension

5.2.1 Purpose

The first goal of the spring tests is to determine the spring constant “k” of the existing spring used in the model. Once this value is obtained it can be compared to the previously calculated rotating spring constant. If the k value of the model spring is greater than or equal to the calculated spring constant, it will be able to overcome the force of the weight due to the tent fly. Additionally, once this k value is within the acceptable range the measured tension force can be marked as reference for the prototype.

5.2.2 Materials

- Spring (from model)
- SolFly model
- Newton-Spring Scale

5.2.3 Procedure

1. Assemble and fixture SolFly model
2. Roll fly until it is completely wound around housing
3. Mark stasis point of spring on PVC tube
4. Pull out the end of fly to arbitrary distance. Record distance
5. Attach Newton-Spring scale to end of fly and hold stationary. Turn scale on and zero it.
6. Lightly tug fly until spring releases and record force on meter.
7. Repeat procedure five times.
8. Use circumference of PVC housing to calculate degrees of rotation of tube.

5.2.4 Data

Dimensions

Length of Spring: 24 cm

Diameter of Spring: 1.5 cm

Circumference of PVC: 12.56 cm

Table 11: Spring data

Force (N)	Distance (cm)	Rotation (Degrees)	Rotation (radians)
9.709	37	1060.51	18.509
8.140	37	1060.51	18.509

8.728	37	1060.51	18.509
7.061	37	1060.51	18.509
7.649	37	1060.51	18.509
8.532	44	1261.15	22.011

5.2.5 Results

Equations used:

$$T = rF \sin(\Theta)$$

$$T = -k\phi$$

Table 12. Results of Spring Constant Test

F (N)	Degrees(Θ)	Torque (Nm)	Radians(ϕ)	k (Nm/rad)
9.709	1060.51	-0.189394	18.509	0.010233
8.140	1060.51	-0.158788	18.509	0.008579
8.728	1060.51	-0.170258	18.509	0.009199
7.061	1060.51	-0.137739	18.509	0.007442
7.649	1060.51	-0.149210	18.509	0.008061
8.532	1261.15	-0.167257	22.011	0.007599
			Avg:	0.008519

5.2.6 Conclusion

Through prior calculations the lowest possible torsional spring constant was found to be $k = 0.00006902 \text{ Nm/rad}$. As shown in table 12, the average k value of the current spring is far above that minimum value. As a result, this data provides confirmation that this spring mechanism is strong enough to overcome the weight of the solar panels and roll up as designed.

Additionally, the tension force should remain within the range of 10-7 N.

5.3 Wind Force on Tent Fly

5.3.1 Purpose

The wind tunnel was used to determine maximum allowable wind speeds on the tent fly. This test was designed such that the scaled tent fly would endure more shear force than the full size product, and was pulled taut to increase the likelihood of ripping. The tent fly was oriented

in the tunnel so that wind force was applied directly to the face of the fly as shown below. Failure of the tent fly was characterized by the tent fabric ripping.

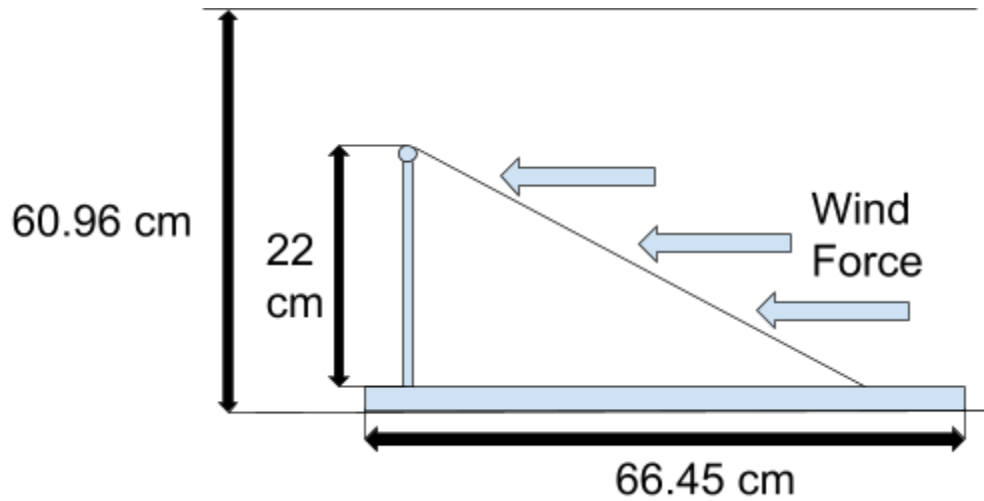


Figure 57: Diagram of Steel Frame with Nylon Fly Fabric Attached inside Wind Tunnel

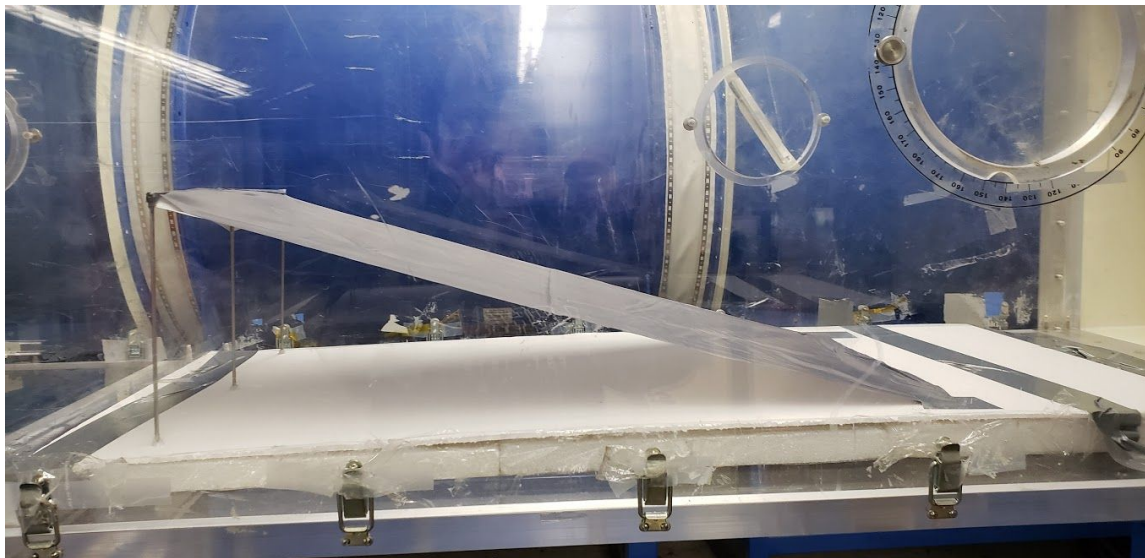


Figure 58: Steel Frame with Nylon Fly Fabric Attached inside Wind Tunnel

5.3.2 Materials

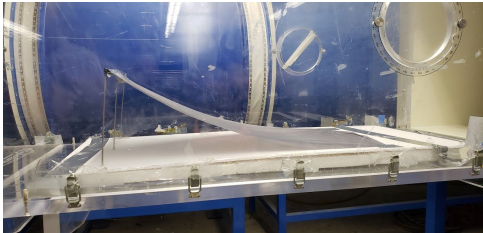
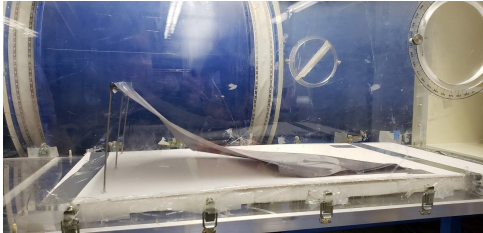
- Wind tunnel
- Tent fly
- Scaled Tent Beams
- Duct tape
- Stopwatch
- Camera

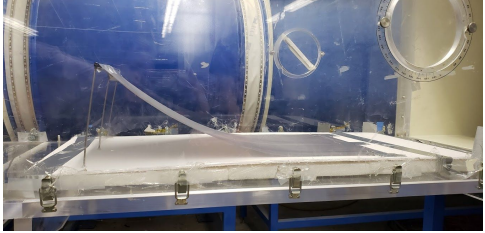
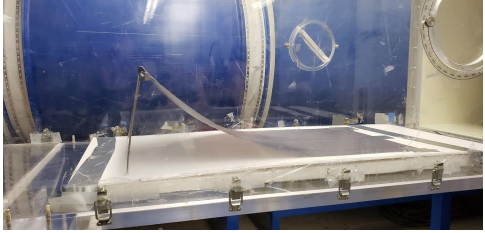
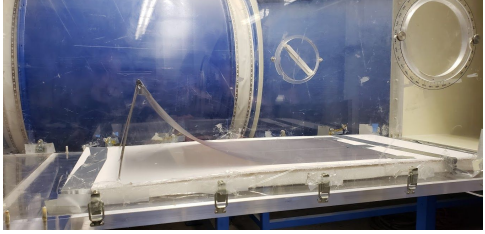
5.3.3 Procedure

1. Attach the fly fabric to the frame, and attach to ground such that the tent fly is pulled taut
2. Place the fly frame into the wind tunnel. Position and fixture the fly frame with tape such that wind flow is directed towards face of fly
3. Turn on the video camera.
4. Set wind tunnel speed to 5 m/s
5. Observe behavior for approximately one minute and record observations.
6. Increase speed in increments of 2-3 m/s and record observations at each speed for a minute.
7. Repeat steps 1 - 7 for each test.

5.3.4 Data

Test 13. Wind Tunnel Data

Speed (m/s)	Failure (Y/N)	Observations	Photo
5	N	Bowed fabric, air seeping in near ground	
7	N	Increase in fabric bow, can see frame shifting	
10	N	Tape tore off. Test restarted from this point. Fabric mostly flat to ground	

10	N	Deeply bowed, fabric & frame shaking	
12	N	Bowed, frame is bending	
14	N	No visible air pockets, same as 12	
15	N	More bending on the frame	

The test was concluded at 15 m/s because poles were bending and the team did not want to cause damage to the wind tunnel.

5.3.5 Results

Data will be used to calculate a factor of safety that can be distributed along with the SolFly to provide consumers at what wind speeds the SolFly should be rolled up and stowed away.

5.3.6 Conclusion

The largest concern is no longer the fabric ripping, but rather the tent frame buckling and bending under wind forces. The team will investigate frame reinforcements for the prototype.

5.4 Electrical

5.4.1 Purpose

The goal of electrical tests is to confirm the model is able produce electricity at a rate matching prior calculations. The model solar panels are tested to confirm functionality of the circuit, and one full size F-WAVE panel is tested to confirm wattage rating. Beginning during peak sunlight hours, both solar devices are tested every half hour until sunlight is no longer available. Recorded voltage and amperage are used to calculate wattage produced at that time. Wattages from tests are compared to desired electrical output.

5.4.2 Materials

- Tent fly
- Tent frame
- Wires
- Sunlight
- Portable phone charger
- Multimeter
- Timer
- F-Wave Solar Panel



Image 59: F-Wave Solar Panel

- Model Solar Circuit

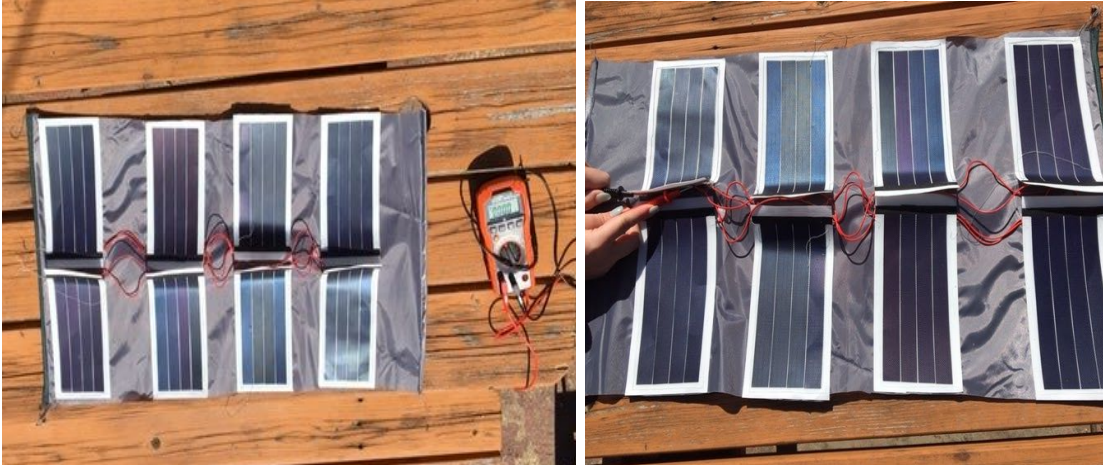


Image 60: model Solar Panel

5.4.3 Procedure

1. Begin test at start of peak sunlight hours based on location and time of year (10:00 am/ 11:00 am in Worcester, MA in March.)
2. Place the full size solar panel and model solar panel flat on ground in unshaded area.
3. Record date, time, and current weather.
4. Using a multimeter, connect test probes to positive and negative terminals of each circuit. Record the voltage and amperage
5. Record voltage and amperage every 30 minutes until end of peak sunlight hours or sunlight is no longer available.
6. Repeat procedure for three separate days.

5.4.4 Data

All recorded data taken with a Klein tools multimeter



Image 61: Klein Multimeter

Table 14. Solar Data Day 1

3/28/2019		Full Size Solar Panel			model Solar Panel		
Time	Weather	Voltage (V)	Amperage (mA)	Watts (W)	Voltage (V)	Amperage (A)	Watts (W)
11:00	Sunny	N/a	N/a	N/a	7.97	1.001	7.98
11:30	Sunny	421	144	60.62	8.01	1.076	8.62
12:00	Partial sun	417.5	154	64.30	7.97	1.115	8.89
12:30	Sunny	422	142	59.92	8.06	1.210	9.75
1:00	Sunny	411	145	59.60	7.94	1.175	9.33
1:30	Sunny	391	118	46.14	8.01	1.190	9.53
2:00	Sunny	392	111	43.51	7.95	1.04	8.27
2:30	Sunny	396	102	40.39	7.97	1.072	8.54
3:00	Sunny	352	38	13.38	7.70	.360	2.77
3:30	Partial sun	352.5	55	19.39	7.77	.497	3.86
4:00	Sunny	375.0	46	17.25	8.03	.635	5.10

Table 15. Solar Data Day 2

3/29/2019		Full Size Solar Panel			model Solar Panel		
Time	Weather	Voltage (V)	Amperage (mA)	Watts (W)	Voltage (V)	Amperage (A)	Watts (W)
10:30	Light rain	285.3	21	5.99	7.28	.225	1.64
11:00	cloudy	310.1	34	10.54	7.68	.324	2.49
11:30	cloudy	341.8	49	16.75	8.03	.558	4.48
12:00	cloudy	350.1	45	18.91	7.68	.511	3.92
12:30	Light rain	302.0	34	10.37	7.39	.296	2.19
1:00	Light rain	294.5	28	8.245	7.45	.279	2.08
1:30	Light rain	211.2	15	3.17	5.66	.122	0.69
2:00	Light rain	237.5	11	2.61	6.36	.150	0.95
2:30	Light rain	335.2	21	7.04	6.18	.150	0.93
3:00	Light rain	219.5	12	2.63	4.30	.073	0.32
3:30	Light rain	182.9	9	1.65	4.86	.076	0.37

Test 16. Solar Data Day 3

3/30/2019		Full Size Solar Panel			model Solar Panel		
Time	Weather	Voltage (V)	Amperage (mA)	Watts (W)	Voltage (V)	Amperage (A)	Watts (W)
11:00	Partial sun	322.5	32	10.32	7.57	.224	1.70
11:30	Partial sun	375.8	77	28.94	7.65	.595	4.55
12:00	Partial sun	367.3	123	45.18	7.76	.692	5.37
12:30	Partial sun	352.2	112	39.45	7.75	.936	7.25
1:00	Partial sun	364.4	83	30.25	7.68	.634	4.87
1:30	Partial sun	336.0	76	25.54	7.42	.450	3.34
2:00	Partial sun	361.4	75	27.11	7.36	.172	1.27
2:30	Partial sun	339.4	51	17.31	7.65	.413	3.16
3:00	Partial sun	348	39	13.57	7.47	.486	3.63
3:30	Mostly Sunny	342.9	41	14.06	7.69	.515	3.96
4:00	Sunny	337.5	47	15.86	7.82	.453	3.54

5.4.5 Results

Recorded voltage and amperage can be used to calculate watts produced at that time by multiplying: $W = V \cdot A$. These values are shown in the table above.

Wattage Produced Daily (F-WAVE Panel)

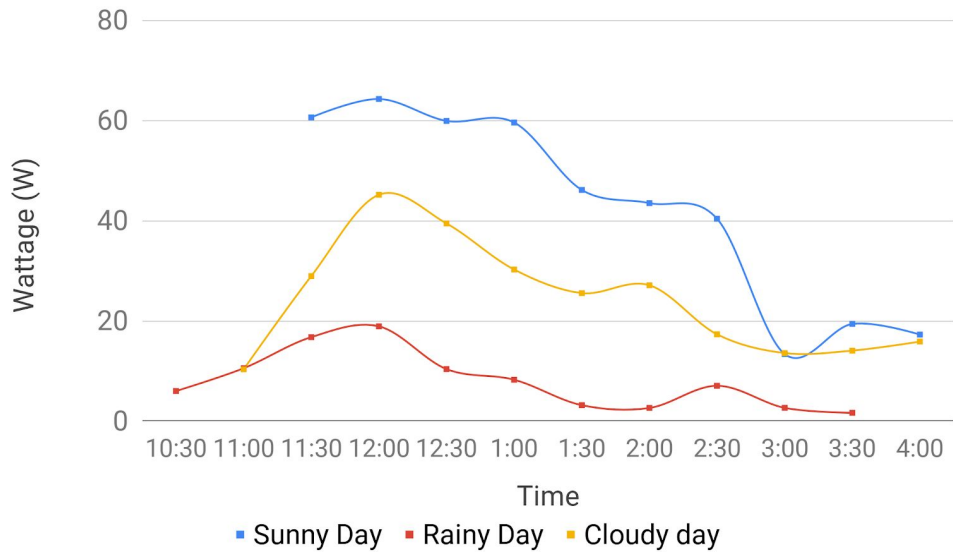


Figure 62: F-WAVE Wattage vs. Time

Wattage Produced Daily (Prototype Circuit Panel)

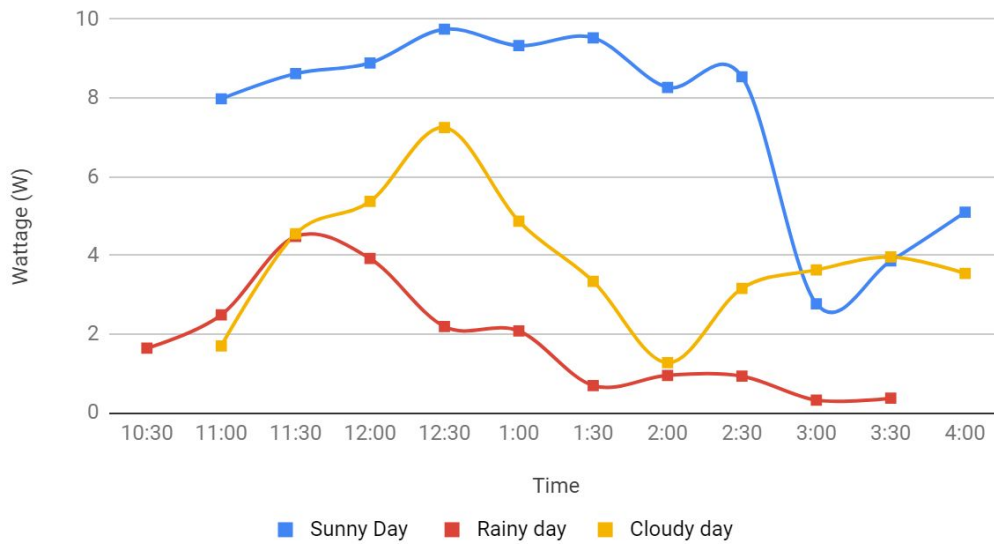


Figure 63: Model Circuit Wattage vs. Time

5.4.6 Conclusion

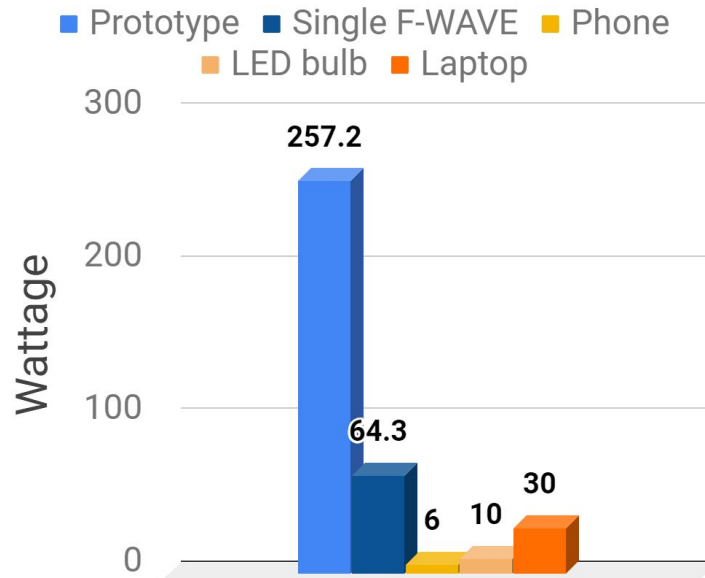


Figure 64: Chart of Wattage Production and Power Requirements of Devices

Results of electrical tests confirmed variations in wattages according to weather conditions as predicted. Maximum wattage produced was 64.3 W at noon on the sunny day. This corresponded with the wattage rating of 70 W. The chart above compares electrical production of the prototype to power requirements for various devices. A single F-WAVE panel could power 6 LED bulbs, and the prototype with four panels could power 25 LED bulbs. It is important to note that average horizontal irradiation in Massachusetts is 3.8 kWh/m² daily compared to the 6.6 kWh/m² daily in Namibia and Jordan. Therefore, electrical production in these regions would be significantly higher.

6.0 Conclusions & Recommendations

SolFly proves to be a feasible solution to energy sparsity in refugee camps. The design successfully met all consumer requirements according to prior market research. These requirements include low cost, transportable, low maintenance, and environmentally friendly. A single SolFly device can be produced for only \$706 and incurs no operational or maintenance costs for up to 10 years. This is a minor expense compared to the \$100 million spent by UNHCR annually on diesel fuel alone [9]. Up to 250 SolFly devices can be transported by a single truck, providing electricity to 250 families per shipment. The spring mechanism makes deployment and storage simple. Solar cells can be cleaned easily by wiping down or rinsing with water. Finally, the SolFly provides 100% green energy. Carbon emissions are harmful to settlement inhabitants and the environment. SolFly creates zero carbon emissions compared to the 14.3 million metric tons of CO₂ emitted by displaced households in 2014 [16].

Based on the location of refugee camps sponsored by the UNHCR, as well as research conducted during this MQP, some suggested locations for SolFly deployment are Namibia and Jordan. These regions have ideal conditions for solar energy production. Irradiation in Namibia and Jordan is 2,200 KWh/m²/year as opposed to the 1,200 KWh/m²/year that is received in Massachusetts [26]. However, SolFly is versatile and can be adapted to meet consumer requirements based on cost and electricity production.

Some precautionary measures must be taken in order to maintain structural integrity of the tent and functionality of the SolFly device. The center beam and three supporting tent poles must be reinforced to avoid deflection due to additional weight. One suggestion for structural reinforcement is increasing the thickness of the poles. By modifying the inner diameter to 20mm, deflection is reduced to nearly zero (0.9945 mm). It is recommended to change the geometry rather than the material, because steel, which is currently used, has high strength and toughness. In addition to tent reinforcement, it is recommended that SolFly be retracted in cases of inclement weather. These conditions include torrential rain and wind speeds exceeding 14 m/s.

Future steps can be taken to further enhance this project. Some tests can be conducted at the scaled model level. The model tent frame with reinforcements and additional weight could be subjected to wind forces in the tunnel to observe behavioral differences. A tensile test could be conducted on the nylon fly to find when it rips. It would be beneficial to make a full scale prototype and test its application in potential target regions. Lastly, the UNHCR should be contacted to propose the product and address price point.

In conclusion, project goals were met and a useful, feasible product was developed. The team experienced the product design process from start to finish. This required application of the engineering knowledge acquired throughout undergraduate studies at WPI. As a self proposed MQP, this project encouraged creative freedom and intellectual development. As a result, there were numerous conceptual pivots and iterations of the product before reaching a satisfactory

final design. The development of SolFly required implementation of design, analysis, and experimental skills. The team was able to apply existing knowledge of software programs such as SolidWorks, and learn new simulation methods using ANSYS. With the combination of engineering skills and topic-specific research, the team was successfully able to create and realize SolFly.



Figure 65: The Team at Project Presentation Day



Figure 66: SolFly Scaled Model

7.0 Works Cited

- [1] Amazon. (2019). Jiang Flexible Solar Panel. Retrieved April 24, 2019, from https://www.amazon.com/stores/page/7EA8E5E4-3D88-44FC-BBAA-05E0C15CB701?store_ref=SB_A05392062BAMMTJ9V1PF6&pf_rd_p=3fade48a-e699-4c96-bf08-bb772ac0e242&hsa_cr_id=3941060820601&lp_slot=auto-sparkle-hsa-tetris&lp_asins=B01JZKF6SQ,B01EY5FIGW,B01MU5UMRF&lp_mat_key=jiang&lp_query=jiang thin film&sb-ci-n=shopNow
- [2] API Solutions. (n.d.). Glossary of Plastic Injection Molding Terms. Retrieved April 24, 2019.
- [3] Curbell Plastics Inc. (2019). Plastics for Outdoor Applications. Retrieved April 10, 2019
- [4] Field Innovation Team. (2018, December 12). DC Do Tank. Retrieved April 24, 2019
- [5] Four Peaks Technologies. (2011). P/N Junctions and Band Gaps. Retrieved March 16, 2019
- [6] Franceschi, J., Rothkop, J., Miller, G. (2014). Off-grid Solar PV Power for Humanitarian Action: From Emergency Communications to Refugee Camp Micro-grids. *Procedia Engineering*, Volume 78, 229-235, ISSN 1877-7058,
- [7] F-WAVE Company Limited. (2015). TECHNICAL DATA. Retrieved February 15, 2019
- [8] Galassi, T. (2015, May 4). Department of Labor logo UNITED STATESDEPARTMENT OF LABOR. Retrieved April 10, 2019
- [9] Green, C. (2018, February 1). 5 Reasons to Care about Refugee Camps. Retrieved January 02, 2019
- [10] Gul, M., Kotak, Y., & Muneer, T. (2016). Review on recent trend of solar photovoltaic technology. *Energy Exploration & Exploitation*, 34(4), 485–526.
- [11] Gutbrod, K. G., Dr. (2019, April 14). Weather Windhoek. Retrieved April 23, 2019
- [12] Hashem, M. (2017, November 14). Jordan's Za'atari camp goes green with new solar plant. Retrieved April 24, 2019

- [13] International Renewable Energy Agency (IRENA). (2018, August 7). Harnessing the power of renewables in refugee camps. Retrieved April 12, 2019
- [14] James Spring & Wire Company. (2017, July 13). Types of Steel Springs and Their Unique Characteristics & Applications
- [15] Lambert, J., Hall, C., Balogh, S., Gupta, A., Arnold, M. (2014). Energy, EROI and quality of life. *Energy Policy*, Volume 64, 153-167, ISSN 0301-4215, <https://doi.org/10.1016/j.enpol.2013.07.001>.
- [16] Lehne, J., Blyth, W., Lahn, G., Bazilian, M., Grafham, O. (2016). Energy services for refugees and displaced people. *Energy Strategy Reviews*, Volumes 13–14, 134-146, ISSN 2211-467X,
- [17] Maurer, C. (2019, February 05). The Best Solar-Powered Camping Gear 2019. Retrieved February 13, 2019
- [18] Ripstop by the Roll. (2019). 1.9 oz PU coated Ripstop Nylon. Retrieved April 10, 2019
- [19] McSweeney, Robert, and Rosamund Pearce. “Interactive: The Impacts of Climate Change at 1.5C, 2C and Beyond.” *Interactive: The Impacts of Climate Change at 1.5C, 2C and beyond | Carbon Brief*, Carbon Brief
- [20] Office of Energy Efficiency & Renewable Energy (EERE). (2013, August 20). Solar Performance and Efficiency. Retrieved February 10, 2019
- [21] Online Home Store for Furniture, Decor, Outdoors & More. (n.d.). Retrieved December 22, 2018
- [22] Plastech Industries Ltd. (n.d.). Retrieved April 24, 2019
- [23] Roberts, T. (2018, November 30). 5 Stunning Prefab Off-grid Homes (with prices). Retrieved March 15, 2019
- [24] Rosenthal, E. (2010, October 4). U.S. Military Orders Less Dependence on Fossil Fuels. *The New York Times*. Retrieved March 1, 2019

[25] Solar Energy Industries Association “Photovoltaic (Solar Electric)”. Retrieved October 12, 2018

[26] National Laboratory for Renewable Energy. (2017, April 4). *Solar Maps: NREL*. Retrieved April 23, 2019

[27] Solargis Solar. (2016, October 13). *Description and Accuracy*. Retrieved April 20, 2019, from Solargis.

[28] Thoubboron, K. (2019, January 02). How Long Does it Take to Install Solar Panels? | EnergySage. Retrieved April 15, 2019

[29] Tortora, P. G., & Merkel, R. S. (2009). *Fairchild's dictionary of textiles* (7th ed.). New York: Fairchild Publications.

[30] Torque Calculation. (n.d.). Retrieved April 4, 2019

[31] UNHCR. *Emergency Handbook*. (n.d.). Retrieved April 23, 2019

[32] UNHCR. (2014). UNHCR Item No 07242. *Family Tent for Hot Climate*, 51-73. Retrieved April 24, 2019

[33] UNHCR. (2018) UNHCR Home

[34] U.S. Department of Energy. (2002). *The History of Solar*[Pamphlet]. Energy Efficiency and Renewable Energy.

[35] Wayfair. (2019). Online Home Store for Furniture, Decor, Outdoors & More. Retrieved April 24, 2019

[36] World Insolation Map. (n.d.)

[37] Wong, W. S., & Salleo, A. (2009). *Flexible electronics: Materials and applications*. Retrieved March 29, 2019

[38] Woodford, C. (2019, January 31). Nylon - The science of synthetic textiles. Retrieved April 15, 2019

[39] NIOSH Lifting Recommendations. (n.d.).